

THESIS FOR THE DEGREE OF LICENTIATE OF ENGINEERING

Investigation of Solid Fuel Conversion in a Fluidised Bed Gasifier
– Modelling and Experiments

LOUISE LUNDBERG

Department of Energy and Environment

CHALMERS UNIVERSITY OF TECHNOLOGY

Göteborg, Sweden 2015

Investigation of Solid Fuel Conversion in a Fluidised Bed Gasifier — Modelling and Experiments

LOUISE LUNDBERG

© LOUISE LUNDBERG, 2015.

Department of Energy and Environment
Chalmers University of Technology
SE-412 96 Göteborg
Sweden
Telephone + 46 (0)31-772 1000

Reproservice
Göteborg, Sweden 2015

Errata sheet

This errata sheet lists errors and their correction for the licentiate thesis of Louise Lundberg, titled “Investigation of Solid Fuel Conversion in a Fluidised Bed Gasifier – Modelling and Experiments”, Chalmers University of Technology, 2015.

Location	Original text	Corrected text
Figure caption for Fig. 2.1, p. 13	Flows into and out of the gasifier of the Chalmers DFBG unit, as well as the direction of discretisation used in the 1D model (grey lines).	Flows into and out of the gasifier of the Chalmers DFBG unit, as well as the direction of discretisation used in the 1D model (grey lines). Modified original material by Erik Sette.
Figure caption for Fig. 3.1, p. 21	Experimental set-up.	Experimental set-up. Modified original material by Placid Atongka Tchoffor.
Figure caption for Fig. 3.2, p. 23	Schematic of the Chalmers indirect gasifier. The combustor and the gasifier are indicated in red and orange, respectively.	Schematic of the Chalmers indirect gasifier. The combustor and the gasifier are indicated in red and orange, respectively. Original material by Anton Larsson.

Investigation of Solid Fuel Conversion in a Dual Fluidised Bed Gasifier – Modelling and Experiments

LOUISE LUNDBERG

Division of Energy Technology
Department of Energy and Environment
Chalmers University of Technology

Abstract

A substantial proportion of Sweden's greenhouse gas emissions originates from the transportation sector, and the Swedish government has set the goal that the entire Swedish vehicle fleet will be independent from fossil fuels by 2030. One of the strategies investigated to achieve this goal is biomass gasification, which is a technology that can be used to transform lignocellulosic materials into a raw gas. This gas can be further upgraded into a transportation fuel, such as substitute natural gas (SNG), Fischer-Tropsch diesel, dimethyl ether, or methanol. Three major techniques can be used for biomass gasification: entrained-flow gasification; single fluidised bed gasification; and dual fluidised bed gasification (DFBG).

This thesis focuses on DFBG with SNG as the end-product. For this process, there is an optimal overall efficiency of SNG production for a certain degree of char conversion in the gasification chamber. The aim of the work of this thesis is to elucidate how the degree of fuel conversion in the gasifier of a DFBG unit is influenced by different parameters. This knowledge is valuable for the design, upscaling, and optimisation of such units.

For this purpose, semi-empirical modelling is combined with experimental work. The model is used to identify the key parameters that affect char gasification in a DFBG unit and to provide the corresponding sensitivity analyses. Furthermore, a general approach for optimising the definition of the conversion classes used in modelling the fuel population balance is proposed and evaluated. Experiments conducted at the laboratory scale examine how the conversion conditions of a fuel particle (fuel vertical mixing, fuel concentration, fuel size, pyrolysis atmosphere, and cooling of the char after pyrolysis) affect the char gasification rate. Experiments are also used to determine the particular kinetic and structural parameters of the biomass fuel used in the Chalmers DFBG unit.

The 1D model, combined with the developed discretisation method for the fuel conversion classes and the experimentally determined kinetic and structural parameters, gave results that were in good agreement with the experimental data for the char conversion degree in the gasification chamber of the Chalmers DFBG unit. Furthermore, the experiments showed

that the position of the fuel during pyrolysis and char gasification had a significant effect on the char gasification rate, for conditions relevant for DFBG. Particle size was also identified as an important parameter. Thus, when carrying out laboratory-scale tests to generate fuel reactivity data to be used for modelling large-scale units, it is important to replicate the conditions experienced by the fuel particles in the large-scale unit and to use similar fuel sizes.

Keywords: gasification, fluidised bed, biomass, modelling, char reactivity, char conversion

List of Publications

This thesis is based on the work presented in the following publications:

- Paper I Lundberg, L., Pallarès, D., Johansson, R., Thunman, H. 2014. A 1-Dimensional Model of Indirect Biomass Gasification in a Dual Fluidised Bed System. In: Proceedings of the 11th International Conference on Fluidized Bed Technology, Beijing, China.
- Paper II Lundberg, L., Johansson, R., Pallarès, D. Thunman, H. 2015. A Conversion Class Model for Describing Fuel Conversion in Large-Scale Fluidised Bed Units. To be submitted.
- Paper III Lundberg, L., Tchoffor, P.A., Pallarès, D., Johansson, R., Thunman, H., Davidsson, K. 2015. Influence of Surrounding Conditions and Fuel Size on the Gasification Rate of Biomass Char in a Fluidised Bed. Revised manuscript submitted to Fuel Processing Technology.
- Paper IV Lundberg, L., Tchoffor, P.A., Johansson, R., Pallarès, D. 2015. Determination of Kinetic Parameters for the Gasification of Biomass Char Using a Bubbling Fluidised Bed Reactor. In: Proceedings of the 22nd International Conference on Fluidized Bed Conversion, Turku, Finland.

Contribution report:

Papers I and II: Main author, responsible for the modelling work.

Papers III and IV: Main author, responsible for the data evaluation and part of the experimental work.

Acknowledgements

First of all, I would like to thank my three (lucky me!) supervisors. Henrik, thank you for all your good ideas and your ability to place everything into its context. David and Robert, thank you for all your help and support, for all our brainstorming sessions, and for helping me to get back on track when I'm lost. And thank you for being good friends.

Malin, thank you for all these years of friendship and for being the best roommate ever. Thank you for all our chats about work and other stuff—it always feels nice to come to work in the morning and to see you at your desk.

Placid, thank you for all your help with the experiments, and for making this modeller feel welcome in a lab!

Thanks to everyone in the gasification group, especially Erik and Anton for providing me with data and for answering all my questions. Also, thanks to the members of the newly started mixed modelling group; I look forward to further cooperation between the research groups. And thanks to everyone at Energy Technology for making it such a nice place to work.

I would also like to express my sincere gratitude to my friends and family, especially to my parents for always believing in me and for supporting me no matter what.

And finally, Simon, my darling, thank you for all our discussions about programming and modelling, for supporting me, and for just being you. I love you more than words can say.

Table of Contents

Abstract	i
List of Publications	iii
Acknowledgements	v
1. Introduction	1
1.1. Aim	2
1.2. Background	2
1.2.1. Dual Fluidised Bed Gasification for SNG Production	2
1.2.2. Parameters Affecting Char Conversion	5
1.2.3. Modelling Char Conversion	7
1.3. Structure of the Thesis	9
2. Modelling	13
2.1. 1D Model	13
2.1.1. Theory	13
2.1.2. Modelled Cases	15
2.2. Conversion Class Model	15
2.3. Particle Model	18
2.4. Char Reactivity Modelling	18
3. Experiments	21
3.1. Laboratory-Scale Experiments	21
3.2. Pilot-Scale Experiments (Chalmers Gasifier)	22
4. Results and Discussion	25
5. Conclusions	33
6. Future Work	35
Notation	37
References	41
Appendix A: Calculation of the Overall Efficiency of the DFBG Process for SNG Production	45

1. Introduction

As a substantial part of Sweden's greenhouse gas emissions (32% in 2013 [1]) originates from the transportation sector, the Swedish government has decreed that the entire Swedish vehicle fleet should be independent from fossil fuels by 2030. One of the options investigated to achieve this goal is biomass gasification, a technology that can be used to transform lignocellulosic materials into a raw gas, which can then be upgraded into a fuel for use in transportation, such as substitute natural gas (SNG), Fischer-Tropsch diesel, dimethyl ether (DME) or methanol [2, 3]. Biomass gasification can also be used to facilitate further integration of biomass into the energy system, e.g., through the production of a gas that has a high calorific value and that can be used in gas engines and turbines [3] or in Integrated Gasification Combined Cycle (IGCC) plants [2].

Biomass gasification can be achieved through: 1) entrained flow gasification (EFG) [3, 4]; 2) single fluidised bed gasification (FBG) [3, 4], also known as direct gasification; and 3) dual fluidised bed gasification (DFBG) [2, 4], also known as indirect gasification. EFG and FBG are autothermal processes in which the heat required for the fuel conversion is provided by combusting part of the fuel. If this is done using air, the calorific value of the product gas is considerably lowered due to the presence of N_2 . To avoid this, pure O_2 can be used, although this adds an additional energy cost that is related to the production of the O_2 [2, 3]. Since DFBG is an allothermal process, heat is provided by circulating the bed material between a combustor and the gasifier. This opens up the possibility of retrofitting fluidised bed boilers into DFBG units; the Chalmers DFBG unit is an example of this [5].

Table 1.1 summarises the main characteristics of the three biomass gasification techniques. To avoid agglomeration and sintering of the bed material, the temperature of the process is restricted for FBG and DFBG, which results in relatively high yields of tars. In contrast, EFG produces relatively low amounts of tar and other by-products. However, since EFG requires very small particles, fuel grinding is necessary. Pressurisation of the system is impractical for DFBG as it consists of two reactors, whereas it is possible for FBG and EFG. Complete fuel burnout, which is achieved in EFG and DFBG, is problematic in FBG.

Table 1.1. Operational conditions, advantages, and disadvantages for EFG, FBG and DFBG [2-4].

	EFG	FBG	DFBG
O₂ production/dilution with N₂	Yes	Yes	No
Maximum temperature	>1600°C*	800°C–1000°C	750°C–1000°C
Yields of tars and by-products	Low	High	High
Fuel grinding required	Yes	No	No
Pressurisation possible	Yes	Yes	No
Fuel burnout	Yes	No	Yes

*High temperatures are required to avoid extensive soot formation [4].

The focus of this thesis is DFBG with SNG as the end-product. For this type of system, there is an optimal overall efficiency for SNG production associated with a certain degree of char conversion in the gasification chamber (see Section 1.2.1). Accordingly, to be able to control the overall efficiency, it is important to understand how the degree of char conversion depends on different factors. This knowledge is also valuable for the design, upscaling, and optimisation of DFBG units.

1.1. Aim

The aim of this work is to gain knowledge about how the degree of fuel conversion in the gasification chamber of a DFBG unit is influenced by different parameters. For this purpose, semi-empirical modelling is combined with experimental work. The linkages between the investigated parameters and the modelling are shown in Fig. 1.4.

The model is used to identify the key parameters that affect char gasification in a DFBG unit and to provide the corresponding sensitivity analyses. In addition, an approach is proposed and evaluated that is valid under all fuel conversion regimes for optimising the definition of the fuel conversion classes used in the fuel population balance.

Experimental work at the laboratory scale is carried out to study how the conditions under which a fuel particle is converted affect the char gasification rate. Experiments are also used to determine the particular kinetic parameters of the biomass fuel used in the Chalmers DFBG unit.

1.2. Background

1.2.1. Dual Fluidised Bed Gasification for SNG Production

The work presented in this thesis is carried out within the framework of the GoBiGas project [6], the objective of which is to use DFBG to produce SNG on a commercial scale (80–100 MW). Three different scales of equipment are currently being used within the

project to improve understanding of the processes that occur within the DFBG system: 1) a laboratory-scale bubbling fluidised bed gasifier [7]; 2) the 2–4-MW Chalmers gasifier [5]; and 3) a 20-MW demonstration plant operated by Göteborg Energi [6].

The principle of DFBG, with its two interconnected fluidised beds, is depicted in Fig. 1.1. Fuel and steam are fed to the gasifier, a bubbling fluidised bed in which drying, pyrolysis, and partial char gasification take place. The remaining char is transported with the circulating bed material into the combustor, which is a circulating fluidised bed unit, where it is combusted with air to generate the heat required by the process (the internal heat demand). If the energy from char combustion does not provide enough heat, it is also possible to recirculate a fraction of the raw gas to the combustor, as shown in Fig. 1.1.

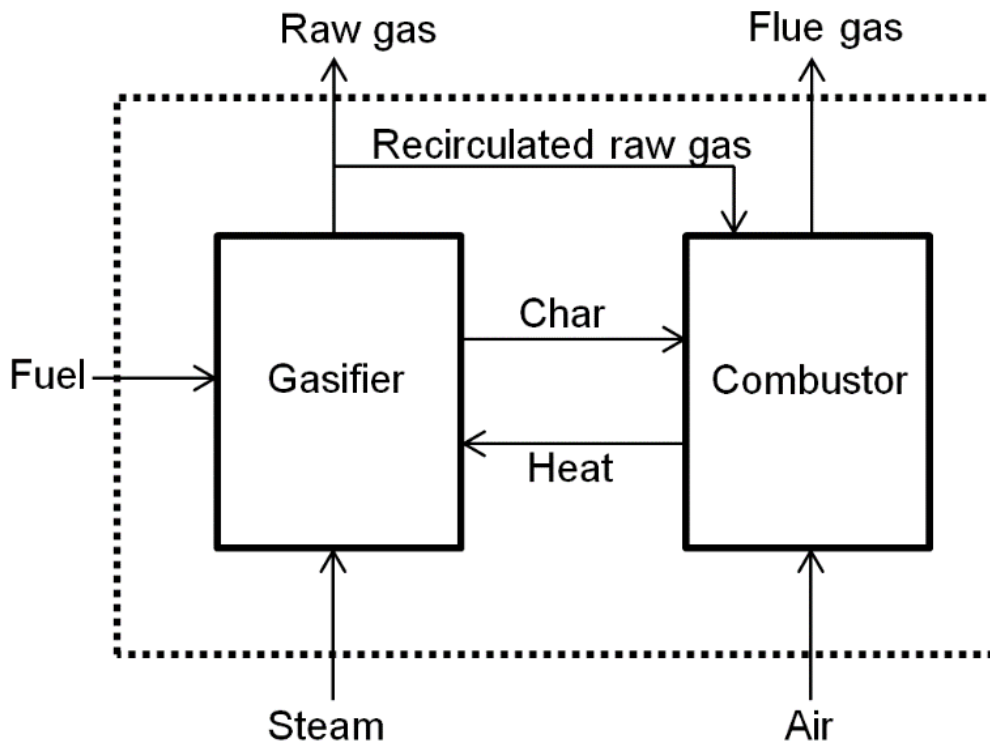


Figure 1.1. Principle of DFBG.

By setting up a heat balance within the system boundaries (indicated by the dotted line in Fig. 1.1), it is possible to calculate the overall efficiency of SNG production, η_{SNG} . It is here assumed that the energy content in the SNG is equal to the energy content of the methane in the SNG (see Appendix A for the detailed calculation). Figure 1.2 shows how the overall efficiency depends on the degree of char conversion in the gasification chamber, w , for three different ratios of H_2/CO in the raw gas (here set as an input for the calculation of η_{SNG}).

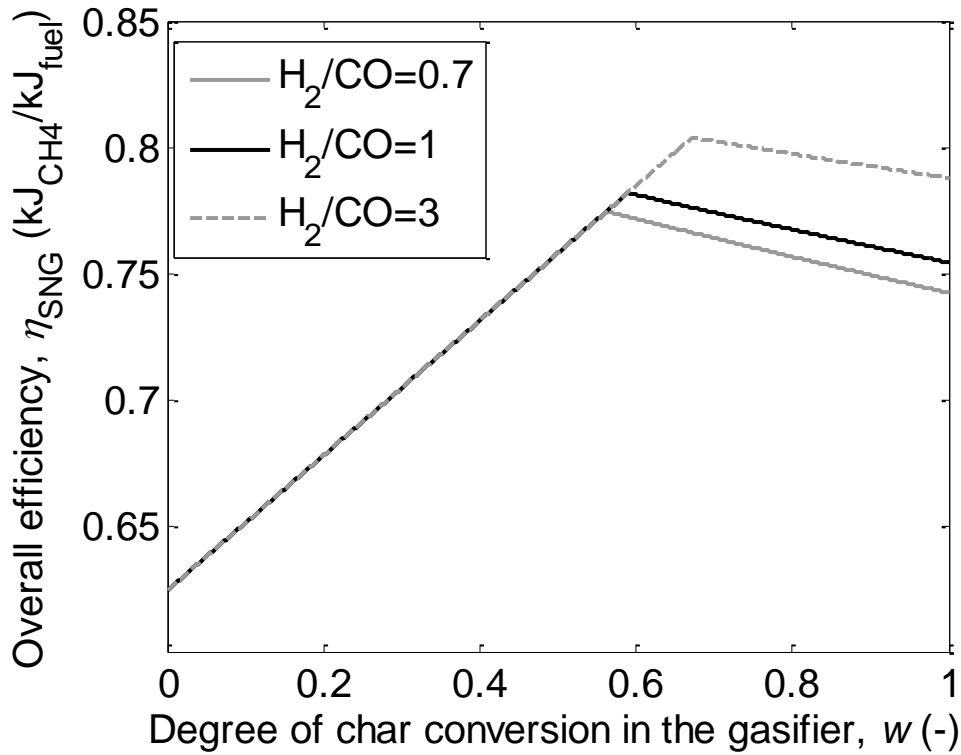


Figure 1.2. Overall efficiency of SNG production as a function of the degree of char conversion in the gasifier, for three different ratios of H_2/CO in the raw gas.

As seen in Fig. 1.2, the overall efficiency initially increases with the degree of char conversion in the gasification chamber, as more of the fuel is converted to gas. At a certain value of w , the heat provided by char combustion exactly matches the internal heat demand (thermal equilibrium), yielding a peak in the overall efficiency. Thus, to the left of the peak, more char is combusted than what is needed to cover the internal heat demand, and cooling is required. To the right of the peak, combustion of a part of the raw gas is necessary to provide the required heat. Recirculation of the raw gas leads to an increase in the internal heat demand (see Appendix A), and this causes the overall efficiency of the process to decrease. The H_2/CO ratio reflects the degree of water-gas shift (WGS) in the gasifier, which affects the internal heat demand. A higher H_2/CO ratio implies a higher degree of WGS and that additional heat is generated by the WGS reaction (Reaction A.5) inside the gasifier. This lessens the need to circulate the raw gas, leading to an increase in the overall efficiency, as seen in Fig. 1.2. The resulting gas compositions for the three cases are given in Fig. 1.3. The dry raw gas is here assumed to consist of CO , CO_2 , H_2 , and CH_4 , although the method described in Appendix A can be expanded to include any number of gas species.

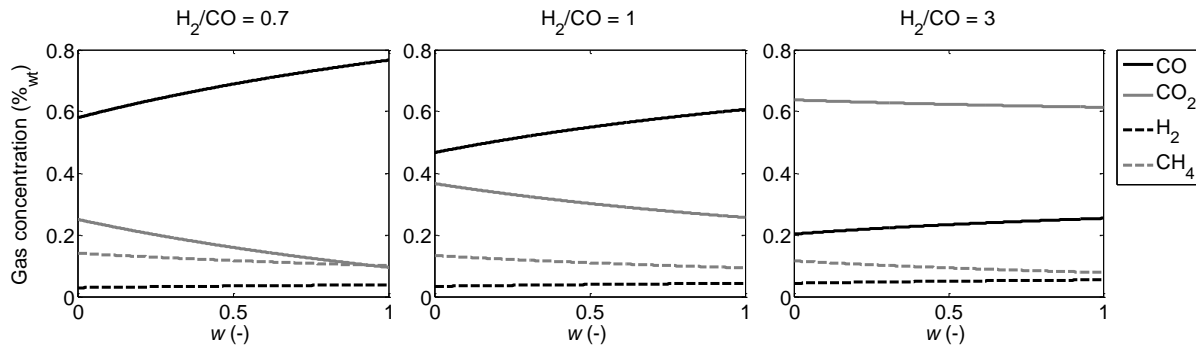


Figure 1.3. Mass composition of the raw gas as a function of the degree of char conversion, w , for three different H_2/CO ratios.

1.2.2. Parameters Affecting Char Conversion

Char can be gasified with H_2O and/or CO_2 according to Reactions 1.1 and 1.2, respectively:



Char gasification is a relatively slow process, which means that for the fuel particle sizes that are typically used in fluidised bed units, the gaseous reactant (H_2O or CO_2) has time to diffuse into the char particle. The rate of char gasification within the particle can vary owing to temperature and/or concentration gradients, and the total surface area and porosity of the particle continuously change as char conversion proceeds [8].

As illustrated in Fig. 1.2, the degree of char conversion in the gasification chamber is important for the optimisation of DFBG, which means that it is crucial to understand its dependence on different factors. Both experiments and mathematical modelling can be useful in this regard. There are many parameters that affect the degree of char conversion in the gasification chamber of a DFBG unit. Some of these are listed in Table 1.2, together with the methods of investigation applied in this thesis. A description of how each parameter affects char conversion in DFBG is given below, as well as a brief review of previous work on the different issues.

Table 1.2. Parameters affecting the degree of char conversion in DFBG.

Parameter affecting char conversion	Method of investigation	Papers
Steam-fuel mixing	Modelling	1
Bed material recirculation	Modelling	1
Char reactivity for H ₂ O gasification	Modelling and experiments	1, 2 & 4
Char reactivity for CO ₂ gasification	Not investigated	-
Gasification atmosphere (mixtures of H ₂ O and CO ₂)	Not investigated	-
Catalytic ash effects	Not investigated	-
Hydrogen inhibition	Not investigated	-
Cooling of char after pyrolysis	Experiments	3
Pyrolysis atmosphere	Experiments	3
Fuel particle size	Experiments	3
Fuel location during pyrolysis	Experiments	3
Fuel location during char gasification	Experiments	3
...	Not investigated	-

The steam-fuel mixing determines the amount of steam that is available for char gasification. Since the fuel particles in a fluidised bed typically reside in the emulsion phase rather than within the bubbles, the steam-fuel mixing is governed by the mass transfer between the bubble phase and the emulsion phase. Experiments in laboratory-scale units show that the mass transfer decreases with increasing bubble size [9].

The recirculation of bed material between the combustor and the gasifier affects the degree of char conversion in two ways. Increased recirculation results in a higher temperature in the gasifier, thereby increasing the conversion rate. However, it also reduces the residence time of the fuel particles in the gasifier, which decreases the degree of conversion. Thus, there exists an optimal mass flow of recirculated bed material that maximises the degree of char conversion in the gasification chamber.

The char reactivity for the reaction with steam (R.1.1) is one of the most important factors for char conversion in DFBG. There are large variations in the reported reactivities of different biomasses. In the review of Di Blasi [10], the activation energy for char gasification with steam ranges from 143 kJ/mole to 237 kJ/mole. This heterogeneity is partly due to difference in composition between different biomasses. In addition, the conditions under which the biomass char is generated affect the reactivity; for instance, chars produced at high heating rates have been found to be 2–3 times more reactive than those produced at low heating rates [11-15]. The steam-char contact during char gasification has also been found to influence the reactivity by affecting the structure of the char [10, 16].

The reactivity of CO₂ gasification of biomass char is several times lower than that of H₂O gasification [17, 18]. For mixtures of CO₂ and H₂O, Nilsson et al. [19] found that the overall reaction rate of char gasification of dried sewage sludge can be approximated by simply adding the gasification rates of CO₂ and H₂O. Ash components (primarily K and Ca) have catalytic effects on the char reactivity [15, 20], whereas H₂ has been observed to inhibit char gasification with H₂O [18, 21, 22]. Cooling the char to room temperature before char gasification can cause the reactivity to decrease by up to 6-fold [17, 23]. The pyrolysis atmosphere (i.e., the fluidising gas during pyrolysis) could also potentially affect the char gasification rate [24, 25].

Diffusional resistances increase with fuel particle size [17], which in turn decreases the gasification rate. In addition, smaller particles have a higher heating rate during pyrolysis than larger particles, which could potentially make smaller particles more reactive. Nilsson et al. [17] investigated the gasification rates of chars derived from sewage sludge in a fluidised bed reactor and they observed that diffusional effects were present for particles with a size of 4.5 mm at 900°C, whereas they did not see an effect of particle size on the char gasification rate at 850°C. However, when investigating the CO₂ gasification of coal char particles and char fines, Li et al. [26] found that the fines had a larger total surface area and thus a higher reactivity than the larger char particles.

The surrounding conditions experienced by the fuel particles vary depending on their vertical position within the fluidised bed, which has been shown to be affected by the fluidisation velocity, u_0 [27]. For low fluidisation velocities, the level of axial particle segregation is high, and the fuel particles are likely to reside at the bed surface. In contrast, higher superficial velocities lead to increased mixing and the fuel particles are, to a greater extent, localised within the dense bed. Thus, it is possible that the operational conditions of a DFBG unit, by affecting the fuel axial mixing, influence the surrounding conditions of a fuel particle (e.g., the heating rate during pyrolysis, the steam-char contact during char gasification, and the fuel concentration), which in turn affect the char reactivity.

1.2.3. Modelling Char Conversion

A model of the gasifier of a DFBG unit can be used for process design, upscaling, and optimisation. Furthermore, such a model can be used to increase understanding of the process through sensitivity studies, as well as to identify key knowledge gaps that require experimental research is.

Models of fluidised bed gasification can be divided into three groups according to their level of detail: computational fluid dynamics (CFD) models; semi-empirical models; and black box models [8]. In CFD models, the momentum balances are solved to acquire the

velocity fields of the gas and solid components, and critical assumptions regarding the interactions between the different phases are required [8]. Semi-empirical models use correlations to estimate the velocity fields, making them less computationally expensive than CFD models. However, their applicability is limited to the conditions that were used when determining the correlations [8]. Black-box models solve the overall, i.e., zero-dimensional, heat and mass balances using empirical correlations. They are thus very simple to use, with very few inputs, but they do not give any information regarding the processes occurring inside the gasifier. As the correlations used are typically only valid for the specific conditions used to determine them, extrapolation of the input variables should be approached with caution [8, 28].

The use of semi-empirical models is still the most commonly applied method for modelling solid fuel conversion in large-scale fluidised beds, as they offer a relatively high level of detail at a reasonable computational cost [8]. Several authors have developed semi-empirical 3D models for solid fuel combustion in fluidised beds [29-31]. For fluidised bed biomass gasification, steady-state 1D modelling is the most common approach [8] (e.g., [32-34]), although there are examples of modelling of gasification in three dimensions [35].

Due to the relatively high level of solids mixing in fluidised beds, fuel particles at different levels of conversion can be present at virtually any location inside the reactor. The most rigorous way to treat this problem is to model the fuel conversion by tracking the location of each fuel particle (or parcel of particles) by solving its equation of motion (Lagrangian Particle Tracking; LPT). LPT, which is often used in a multiphase CFD framework, has been applied to CFB combustion and BFB gasification [36-39]. A less detailed approach is to assume constant conversion rates for each stage of fuel conversion and solve one mass balance for each of the three corresponding fuel components (moisture, volatiles and char). Constant rates obtained from correlations are commonly used in 0D models, in which the concentration field of the fuel particles is not solved [28]. This method has also been used for modelling drying and pyrolysis/devolatilisation in 3D models, combined with population balance modelling (see below) for char conversion [31].

A method that is more affordable (in terms of computational cost) than LPT and that offers a higher level of detail than the use of constant rates is to solve the fuel population balance. In this approach, the fuel conversion process is divided into several fuel conversion classes with different conversion rates, and one mass balance is solved for each conversion class. The use of population balances is the most commonly applied method to model solid fuel conversion in holistic models of large-scale CFB boilers [29-31, 40]. For FB gasifiers, population balances are used less commonly [8, 41].

The discretisation of the conversion process is usually based on the fuel particle size, and a shrinking sphere model is used to describe the fuel conversion of a single particle [29, 31, 40]. This approach is appropriate when the conversion takes place under the shrinking sphere regime, which is typical for char combustion where the reaction rate is high compared to the rate of diffusion of O₂ into the particle [8]. Likewise, when conversion takes place in the shrinking density regime, density classes can be used. However, when there are temperature and/or concentration gradients within the fuel particle, which is often the case for char gasification and for the drying and devolatilisation of large fuel particles, an alternative discretisation method is needed.

1.3. Structure of the Thesis

This thesis summarises and links the modelling and experimental work described in the four attached papers. Figure 1.4 shows how the papers and the chapters/sections of the thesis (indicated in bold font) are connected to the modelling and experimental work and, thereby, to the aim of increasing the understanding of how fuel conversion in the gasification chamber of a DFBG unit is affected by various parameters.

Figure 1.4 also illustrates how the parameters that affect the fuel conversion are investigated in this work, with the four papers in focus. The arrows in Fig. 1.4 indicate how the different parameters are connected to each other and to the models and the experimental work. The solid arrows describe connections that are investigated in this work (black, through modelling; grey, with experiments). The dashed lines represent connections that are included in the model but whose effects remains to be investigated. The dotted lines indicate connections that have not been explicitly examined in the present work and that have not yet been incorporated into the model.

The one-dimensional model for the bottom bed of the gasifier in a DFBG system (denoted the ‘1D model’) is described in Paper 1 and in Section 2.1 of this thesis. As described in greater detail in Sections 2.2–2.4, the fuel conversion within the 1D model was modelled using either: a) the shrinking sphere model (Paper 1); or b) a conversion class distribution based on a particle model (Paper 2), which was developed to increase the accuracy of the 1D model. In Paper 2, a method for dividing the fuel conversion process into conversion classes is proposed and evaluated regarding its ability to minimise the computational cost of the fuel population balance used in the 1D model.

The conducted experimental work consists of two parts: 1) an investigation of the effects on the char gasification rate of various parameters, such as the fuel concentration and the fuel vertical mixing (Paper 3 and Chapter 3); and 2) the determination of the char reactivity of the fuel used in the Chalmers gasifier, combining kinetic parameters with a structural model (Paper 4, Section 2.4, and Chapter 3). The resulting char reactivity model was subsequently incorporated into the particle model (Paper 2).

2. Modelling

2.1. 1D Model

2.1.1. Theory

The semi-empirical 1D model, developed for the dense bottom bed of the gasification chamber of a DFBG unit, discretises the reactor along a single lateral direction (that of the solids cross-flow). The considered mass and energy flows into and out of the gasifier, as well as the direction of discretisation are indicated in Fig. 2.1.

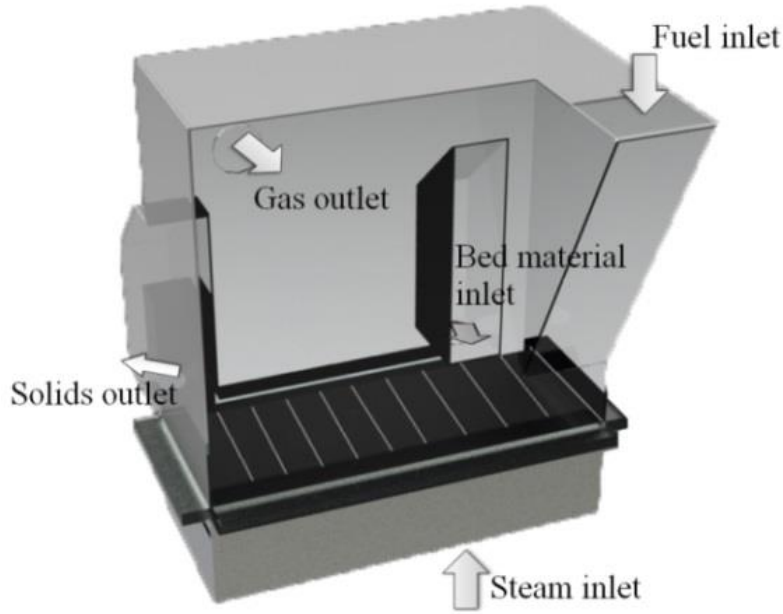


Figure 2.1. Flows into and out of the gasifier of the Chalmers DFBG unit, as well as the direction of discretisation used in the 1D model (grey lines).

The model includes a heat balance [Eq. (2.1)] and mass balances of the different gas species considered for the bubble and the emulsion phase [Eqs. (2.2) and (2.3), respectively], the bulk solids [Eq. (2.4)] and the conversion classes of the fuel components [Eq. (2.5a)].

$$0 = -C_{p,BM} \frac{d}{dx} (u_{BM} \rho_{BM} T) - \sum_k \frac{d}{dx} (\theta u_{BM} \rho_k h_k) \quad (2.1)$$

$$+ \sum_k \frac{d}{dx} \left((D_F h_k) \frac{d\rho_k}{dx} \right) + \frac{d}{dx} \left((k + k') \frac{dT}{dx} \right) + \frac{d}{dx} \left(\sum_i \left(D_G h_i \rho_{G,e} \frac{dY_{e,i}}{dx} \right) \right) + S_E$$

$$0 = K_{be} (\rho_{G,e} Y_{e,i} - \rho_{G,b} Y_{b,i}) + S_{b,i} \quad (2.2)$$

$$0 = \frac{d}{dx} \left(D_G \rho_{G,e} \frac{dY_{e,i}}{dx} \right) + K_{be} (\rho_{G,b} Y_{b,i} - \rho_{G,e} Y_{e,i}) + S_{e,i} \quad (2.3)$$

$$0 = \frac{d}{dx} \left(D_{BM} \frac{d\Phi_{BM}}{dx} \right) + S_{BM} \quad (2.4)$$

$$0 = -\frac{d}{dx} (\theta u_{BM} \rho_{k,j}) + \frac{d}{dx} \left(D_F \frac{d\rho_{k,j}}{dx} \right) + S_{k,j} \quad (2.5a)$$

The energy balance [Eq. (2.1)] includes convective and dispersive heat transfer by the bed material and the fuel components, conductive heat transfer, heat transfer by dispersion of the different gas components, and source terms of the energy flows into and out of the gasifier.

The classical two-phase model approach [42] is used to describe the gas flow. It is based on the assumption that all the solid material and some of the gas resides in the emulsion phase, in which the superficial gas velocity is equal to the minimum fluidisation velocity, u_{mf} . The excess gas fed to the bed, i.e., that corresponding to a volumetric flux of $u_0 - u_{mf}$, passes through the bed in the bubble phase. Thus, for each gas species, two mass balances are formulated that correspond to the bubble phase [Eq. (2.2)] and the emulsion phase [Eq. (2.3)]. Mass transfer between the bubble phase and the emulsion phase is governed by the bubble-emulsion interchange coefficient, K_{be} , whereas lateral gas transport within the emulsion phase is governed by the gas dispersion coefficient, D_G . (Fig. 2.2). The source terms in Eqs. (2.2) and (2.3) include the WGS reaction and transport into and out of the gasifier, i.e., the gas entering the reactor and that leaving at the bed surface.

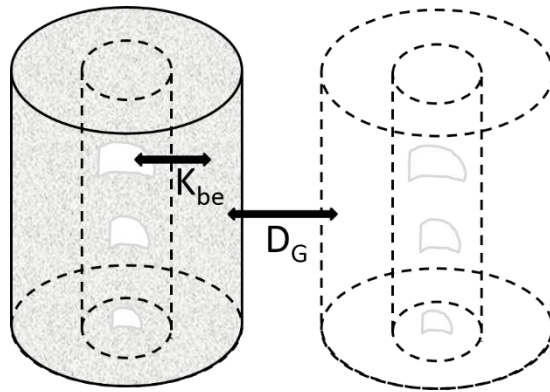


Figure 2.2. Mass transfer of gas species between the bubble phase and the emulsion phase, as well as within the emulsion phase.

In Eq. (2.4), it is assumed that the transport of bed material occurs through dispersive lateral mixing. By solving the potential flow function in Eq. (2.4), Φ_{BM} , the velocity field induced by the cross-flow of bed material can be calculated with Eq. (2.6) [43]:

$$u_{BM} = \frac{D_{BM}}{\rho_{BM}} \left(\frac{d\Phi_{BM}}{dx} \right) \quad (2.6)$$

The reactive fuel components (moisture, volatiles and char, or the entire ash-free fuel) are each divided into a number of conversion classes (see Section 2.2) and Eq. (2.5a) is solved for each class j of fuel component k . Equation (2.5a) includes convective and dispersive mass transport, as well as a source term that includes reactions and transport into and out of the gasifier. Equation (2.5a) is also used to calculate the concentration field of ash within the gasifier, using only one class and no reaction terms. In Paper 1, constant conversion rates were assumed for moisture and volatiles, and Eq. (2.5a) was solved for only one class for each of these fuel components. More details regarding the 1D model and Eqs. (2.1–2.6) can be found in Paper 1.

2.1.2. Modelled Cases

In Chapter 4, two different cases are considered: 1) a case that uses the dimensions and input data for the Chalmers gasifier [5], for which the degree of char conversion is relatively low (see Section 3.2); and 2) a case that uses a reactor that is three times longer but that has the same mass flow of steam for fluidisation, yielding a lower fluidisation velocity, and thereby lower values for the fuel dispersion coefficient [4] and the cross-flow impact factor [4]. This results in a longer residence time for the fuel and consequently, a higher degree of char conversion in the gasifier. The differences in input data between the two cases are given in Table 2.1.

Table 2.1. Input data for the two cases investigated in Chapter 4.

	Chalmers gasifier	Larger gasifier
Length of gasifier	$L_{Chalmers}$	$3 \cdot L_{Chalmers}$
Fluidisation velocity (m/s)	0.3	0.1
Dispersion coefficient (m²/s)	0.002	0.001
Cross-flow impact factor (-)	0.8	0.1

In this work, the 1D model is used to perform a sensitivity analysis of how different input parameters affect the degree of char conversion in the gasification chamber of the Chalmers DFBC unit, as indicated by the solid black arrows in Fig. 1.4.

2.2. Conversion Class Model

Equation (2.5a) can also be written in the form of a population balance, for all fuel components, k , according to:

$$\left\{ \begin{array}{l} \text{rate of mass} \\ \text{accumulation} \\ \text{of class } j \end{array} \right\} = \left\{ \begin{array}{l} \text{incoming} \\ \text{mass flow} \\ \text{of class } j \\ \text{from} \\ \text{adjacent} \\ \text{cells} \end{array} \right\} - \left\{ \begin{array}{l} \text{outgoing} \\ \text{mass flow} \\ \text{of class } j \\ \text{to adjacent} \\ \text{cells} \end{array} \right\} + \left\{ \begin{array}{l} \text{mass flow} \\ \text{entering} \\ \text{class } j \text{ from} \\ \text{class } j - 1 \end{array} \right\} - \left\{ \begin{array}{l} \text{mass flow} \\ \text{leaving} \\ \text{class } j \text{ for} \\ \text{class } j + 1 \end{array} \right\} \quad (2.5b)$$

In Eq. (2.5b), the term on the left-hand side (LHS) designates the rate of mass accumulation of fuel component k of conversion class j within a computational cell. In this work, the focus is on steady-state conditions, so the term on the LHS of Eq. (2.5b) is set to zero. The first two terms on the right-hand side (RHS) describe the convective and dispersive flows of class j . The third term on the RHS describes how fuel component k of class $j-1$ (i.e., a class of a lower degree of conversion) enters class j due to conversion, whereas the fourth term on the RHS designates the amount of fuel component k that leaves class j for a higher class, $j+1$, as it is converted.

In Paper 1, the fuel conversion process was assumed to follow the shrinking sphere model, which implies the definition of size-based conversion classes. However, as discussed in Section 1.1.3, when there are concentration and/or temperature gradients within a fuel particle a more general discretisation approach is required. The conversion class model developed in Paper 2 is instead based on the degree of conversion, and is thus applicable to all conversion regimes.

Figure 2.3 shows the principle of the conversion class model. Here, $\dot{m}_{l,k}$ designates the mass flow of fuel component k that has reached a certain degree of conversion, $X_{j+1,k}$, and thus leaves class j for class $j+1$.

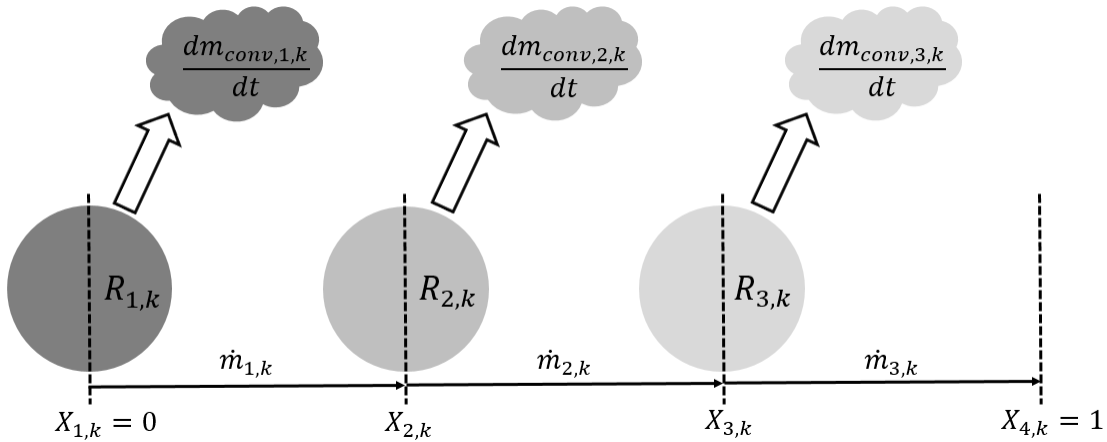


Figure 2.3. Principle of the conversion class model for three classes.

The mass flow of fuel component k leaving class j is given by:

$$\dot{m}_{j,k} = \frac{dm_{conv,j,k}}{dt} \frac{(1 - X_{j,k})}{(X_{j,k} - X_{j+1,k})} \quad (2.7)$$

A particle model (Section 2.3) is used to simulate the conversion of a single fuel particle, which results in conversion rates that vary with the degree of conversion. These conversion rate curves can be discretised, yielding a number of conversion classes, for which each class has an individual conversion rate. Figure 2.4a shows the degree of conversion of volatiles as a function of time, as given by the particle model, χ_k , and a linear approximation of the conversion, $X_{lin,k}$, given by discretising the process into three equally large classes, $\Delta X_k = 33\%$. The shaded area, $A_{l,k}$, is a measurement of the error of class $j = 1$.

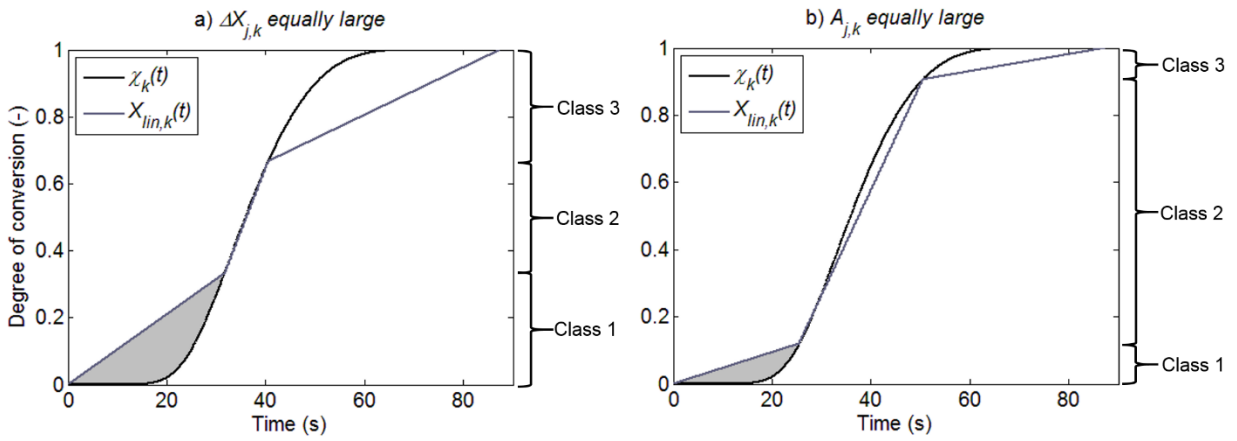


Figure 2.4. Degree of conversion of volatiles as a function of time (for a bed temperature of 800°C) for the particle model (black curves) and a linear approximation (grey curves) using: a) three equally large classes; and b) three classes with the same error. The shaded area represents the error of the linear approximation.

As seen in Fig. 2.4a, when three equally large classes are used, the value of $A_{j,k}$ becomes considerably higher for classes 1 and 3 than for class 2, resulting in a poor description of the conversion process. In order to decrease the error and to distribute it uniformly along the conversion process, the areas between the curves for each class need to be of similar magnitude. In Paper 2, a discretisation method, which is based on assigning the same value of $A_{j,k}$ to all the classes, is described and evaluated, and the conversion class model is thereafter incorporated into the 1D model. Figure 2.4b shows the linear approximation of the conversion process given by this method.

2.3. Particle Model

The particle model is discretised in space (1D) and time. It solves the energy and gas species transport equations taking into account the drying, pyrolysis, char conversion, and shrinkage of the particle. Models presented in the literature are used to describe drying and pyrolysis [44], whereas the char reactivity model and its corresponding kinetic and structural parameters are taken from Paper 4. Mass and heat boundary conditions for large active particles in a fluidised bed have been used [45]. More details about the particle model are given in Paper 2.

2.4. Char Reactivity Modelling

In Paper 1, char gasification is assumed to take place in the shrinking sphere regime. The efficient char gasification rate, which includes both the diffusion of water vapour from the surroundings to the particle surface and the kinetics, is modelled according to:

$$k_{rc,eff} = \frac{k_{rc}h_m}{k_{rc} + h_m} \quad (2.8)$$

The kinetic rate constant, k_{rc} , and the mass transfer coefficient, h_m , are given by Eq. (2.9) [46] and Eq. (2.10) [47], respectively:

$$k_{rc} = 10^{(0.2 \cdot 10^{-4} E_a + 2)} e^{-E_a/(RT)} \quad (2.9)$$

$$Sh = \frac{h_m d_P}{D_{AB}} = (2 + 0.6 Re^{0.5} Sc^{1/3}) \quad (2.10)$$

In Chapter 4, two different activation energies, 128 kJ/mole and 158 kJ/mole, are tested to calculate the kinetic rate constant according to Eq. (2.9), yielding a “High” and a “Low” reactivity biomass, respectively [21, 46].

In the literature, structural models have often been used to describe how the rate of char gasification changes with the degree of char conversion [8]. Paper 4 includes an investigation of how well three structural models fit the experimental data for char gasification of wood pellets (the fuel used in the Chalmers gasifier) in a laboratory-scale fluidised bed reactor. The reactivity model for char gasification used in Paper 4 is written according to Eq. (2.11) [48], assuming n^{th} order kinetics:

$$R_m = k_0 e^{\frac{-E_a}{RT}} P_{H_2O}^n f(X) \quad (2.11)$$

Here, X is the degree of conversion, given by:

$$X(t) = \frac{m_{c,0} - m_c(t)}{m_{c,0}} \quad (2.12)$$

R_m in Eq. (2.11) is the reactivity normalised with the initial mass of char:

$$R_m = \frac{dX(t)}{dt} = -\frac{1}{m_{c,0}} \frac{dm_c(t)}{dt} \quad (2.13)$$

The three structural models, $f(X)$, tested in Paper 4 are: the grain model [49]; the random pore model [50]; and an empirical model [17] (Table 2.2). The empirical model was implemented in the particle model (Paper 2) to describe char conversion.

Table 2.2. Structural models tested in Paper 4.

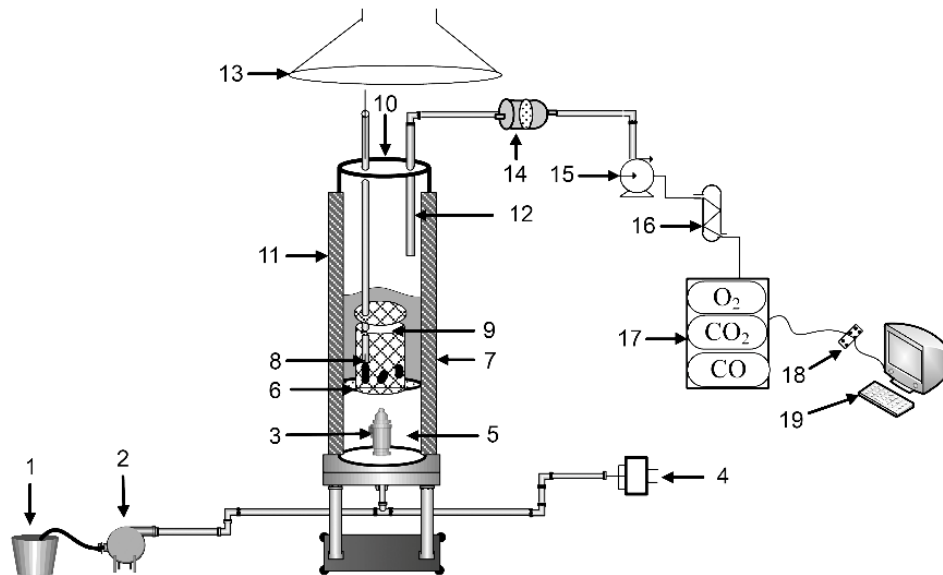
Structural model	f(X)	Parameters
Grain model (GM)	$(1 - X)^{2/3}$	-
Random pore model (RPM)	$(1 - X)\sqrt{1 - \psi \ln(1 - X)}$	ψ
Empirical model (EM)	$(1 - X)(aX + b)\exp(-cX^d)$	a, b, c, d

3. Experiments

3.1. Laboratory-Scale Experiments

The aims of the experimental work presented in this thesis were to: 1) investigate the effects on the char gasification rate of the fuel size and the surrounding conditions of the fuel particles (Paper 3); and 2) determine the char reactivity of the fuel used in the Chalmers unit (Paper 4). Figure 1.4 illustrates how these laboratory-scale experiments are linked to the modelling (solid grey arrows) and thus to the aim of increasing the understanding of how different parameters affect the degree of char conversion in the gasification chamber of a DFBG unit.

A laboratory-scale bubbling fluidised bed reactor with an inner diameter of 7 cm was used in the experiments. The experimental set-up is presented in Fig. 3.1. The bed, which consisted primarily of silica sand, was fluidised with a mixture of H₂O and N₂ fed into the bed through a perforated ceramic plate. The reactor temperature was controlled by heating elements on the reactor walls. A slipstream of the gas mixture was extracted from the reactor using a gas probe, whereas the remaining gas exited through an exhaust hood. The extracted gas was transported through a particle filter and a condenser before reaching the gas analysers, where the concentrations of CO, CO₂, and O₂ were measured and logged on a computer.



1-water tank, 2-water pump, 3-inbuilt steam generator, 4-mass flow regulator, 5-gas preheater, 6-perforated ceramic plate, 7-sand bed, 8-thermocouple inserted into pellet, 9-wire-mesh basket, 10-fuel inlet when basket is not used, 11-heating elements, 12-gas probe, 13-exhaust hood, 14-particle filter, 15-gas pump, 16-condenser, 17-gas analysers, 18-PC logger, 19-computer

Figure 3.1. Experimental set-up.

The fuel particles could either be dropped into the bed from the top of the reactor and move freely inside the reactor (“free”, *F*) or be placed inside a wire-mesh basket. The basket was inserted into the reactor at one of the following locations: 1) completely covered by the dense bed (“inside bed”, *IB*); or 2) in a position such that the fuel particles mainly resided at the bed surface (“bed surface”, *BS*). As pyrolysis and char gasification were separated in time in the experiments, char gasification was not inhibited by volatile species. Thus, the observed gasification rates correspond to the maximum gasification rates that can be achieved in the gasification chamber of a DFBG unit, in the volatile-free areas far from the fuel-feeding ports.

The wire-mesh basket was used to investigate the effect on the char gasification rate of the axial location of the fuel during pyrolysis and char gasification (Paper 3). Five different combinations of the fuel axial location were investigated (Table 3.1), using wood pellets (WP) or wood chips (WC) as the fuel. In some of the experiments with wood pellets, the pellets were cooled prior to char gasification, which allowed estimation of the char yield as well as investigation of the effect of cooling on the char gasification rate. Brunauer–Emmett–Teller (BET) surface analysis with N₂ was carried out on char samples that were extracted from the reactor after char gasification.

Table 3.1. Fuel axial locations investigated in Paper 3.

Pyrolysis	Char gasification
F	F
IB	IB
IB	BS
BS	IB
BS	BS

Abbreviations used: F, free inside the reactor;
IB, inside the bed; BS, at the bed surface.

The influences of the pyrolysis atmosphere, fuel size, and number of pellets were investigated without the use of the basket. The experiments aimed at determining the kinetic parameters of the biomass used in the Chalmers unit (Paper 4) were also carried out without the basket.

3.2. Pilot-Scale Experiments (Chalmers Gasifier)

A schematic of the Chalmers indirect gasifier is shown in Fig. 3.2, with the combustor (a 12-MW CFB) and the gasifier (a 2–4-MW BFB) indicated in red and orange, respectively. Some characteristic operational parameters and geometry data are given in Table 3.2.

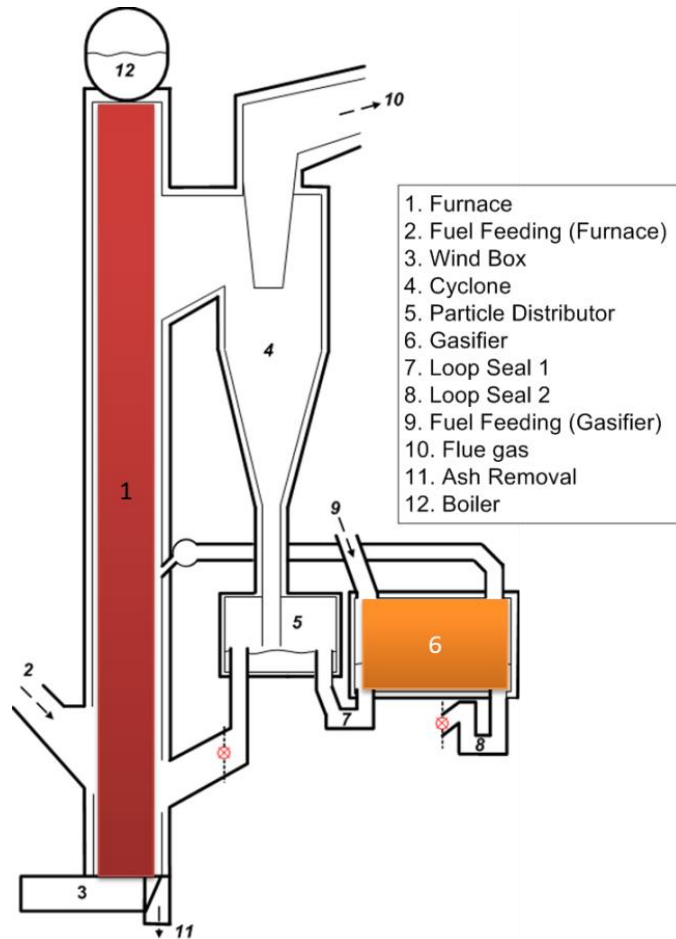


Figure 3.2. Schematic of the Chalmers indirect gasifier. The combustor and the gasifier are indicated in red and orange, respectively.

Table 3.2. Geometry and characteristic operational parameters of the Chalmers indirect gasifier.

Parameter	Value
Cross-sectional area of gasifier (m ²)	1.44
Bed height (m)	0.4–0.6
Bed material (-)	Sand, olivine
Bed material recirculation (kg/s)	4.0–6.5
Fuel (-)	Wood pellets, wood chips
Fluidisation medium, gasifier (-)	Steam
Fluidisation velocity, gasifier (m/s)	0.1–0.3

In Chapter 4, an experimental measurement of the degree of char conversion in the Chalmers gasifier is used to validate the 1D model. The value, 2% (with an experimental error range of 0%–10%), was determined in the work of Larsson et al. [5].

4. Results and Discussion

The most important findings from the four papers are presented and discussed in this chapter. For the results presented here, the focus is on how the fuel conversion, and in particular the degree of char conversion, is affected by different parameters. Figure 4.1 illustrates the effects of the bed material recirculation, the gas-solids mixing, and the fuel reactivity on the degree of char conversion, as calculated using the 1D model described in Paper 1. An experimental value from the Chalmers gasifier is also shown (2% [5], see Section 3.2), as well as the uncertainty related to this measurement. Three different values of the bubble-emulsion interchange coefficient, K_{be} [cf. Eqs. (2.2) and (2.3)], were used to describe the mass transfer between the bubble phase and the emulsion phase. Two biomass reactivities (“High” and “Low”; see Section 2.4) were investigated.

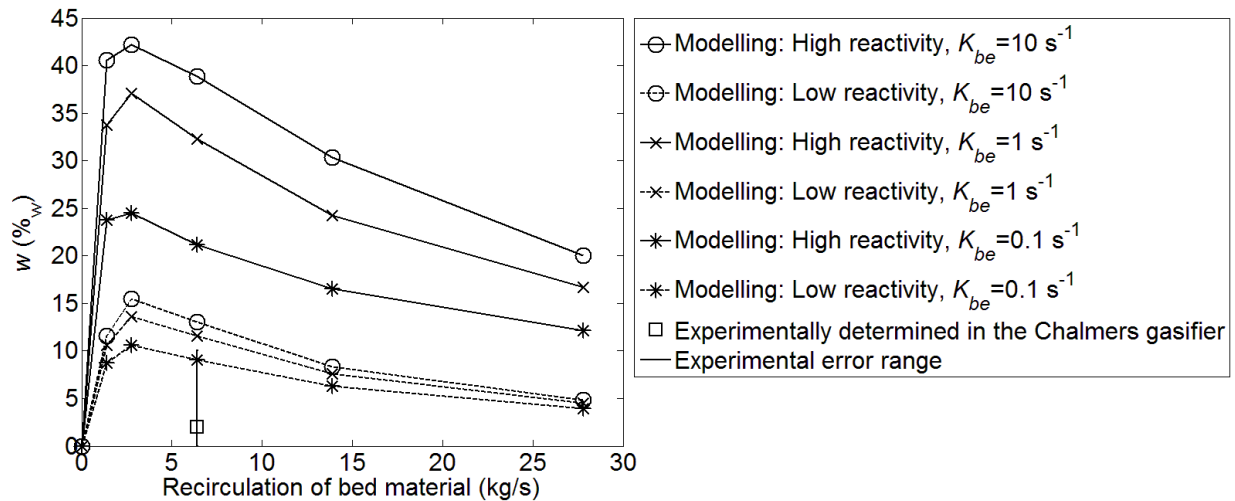


Figure 4.1. Degree of char conversion as a function of bed material recirculation rate, for different reactivities and bubble-emulsion interchange coefficients.

As expected, a peak occurs in the degree of char conversion at a certain bed material circulation rate for all the investigated cases, due to the trade-off between the increase in bed temperature and the decrease in residence time of the fuel, as discussed in Section 1.2.2. The K_{be} value has a relatively strong impact on the degree of char conversion at high fuel reactivities, whereas the impact is weaker when the reactivity is lower.

As seen, the biomass reactivity strongly affects the degree of char conversion. It should be noted that for the range of biomass reactivities investigated and with the size class model used to calculate the degree of char conversion in Fig. 4.1, the 1D model is unable to predict

the experimental value of 2% from the Chalmers gasifier, even when low K_{be} values are used. As discussed in Section 1.2.2, the reactivity of a biomass char depends on both the fuel composition and the conditions under which it is generated and gasified. Thus, considering this and the results from Fig. 4.1, it is possible to conclude that when modelling the gasification of biomass char, it is inappropriate to apply kinetic parameters from the literature to conditions and biomasses for which these parameters were not determined.

The determination of the kinetic parameters for the gasification of wood pellets is described in Paper 4. Figure 4.2 shows a comparison of the experimental reactivity and the modelled reactivities for steam gasification at 758°C and $X_{H_2O} = 89\%_{vol}$, using the three structural models given in Table 2.2. As is evident in Fig. 4.2, only the empirical model can reproduce the experimental reactivity in a satisfactory manner.

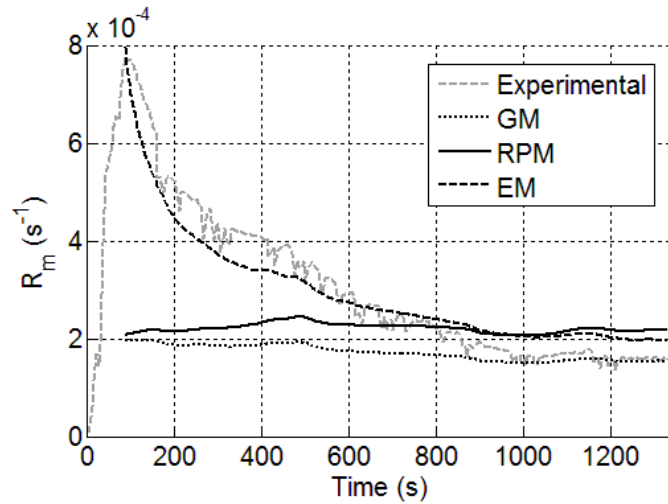


Figure 4.2. Experimental reactivity compared to the reactivities modelled using the grain model (GM), the random pore model (RPM), and the empirical model (EM).

As seen, none of the structural models are able to predict the initial part of the conversion process (approximately corresponding to $X < 5\%$). For $X < 5\%$, $f(X)$ in the particle model (Paper 2) is set to a constant value, namely $f(X = 5\%)$.

In order to investigate whether or not the operational conditions of a DFBG unit can influence the degree of char conversion in the gasification chamber, the effects of the axial positions of the fuel during pyrolysis and char gasification on the char gasification rate of wood pellets (WP) and wood chips (WC) were examined in Paper 3. The results are given in Fig. 4.3, where the error bars include uncertainties regarding the char yield and the gas analysers. It is clear that the WP and WC have similar gasification rates, although there is a rather large uncertainty associated with the gasification rate of the WC, which is

attributable to the fact that the char yield of the WC had to be assumed. As seen, cooling the WP char after pyrolysis decreased the gasification rate somewhat (8–33%).

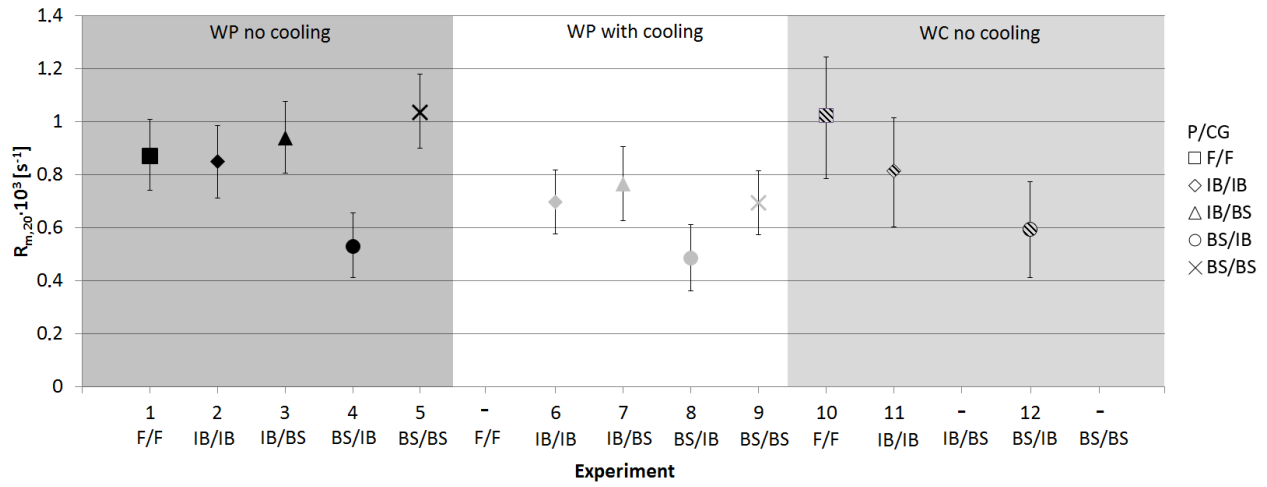


Figure 4.3. Char gasification rates at a char conversion degree of $X = 20\%$ in Exps. 1–12. WP, wood pellets; WC, wood chips; P, pyrolysis; CG, char gasification; F, free within the gasifier; IB, inside the dense bed; BS, on the bed surface.

As is evident from Fig. 4.3, the case labelled BS/IB (pyrolysis on the bed surface and char gasification inside the dense bed) has a significantly (1.6–2.0 times) lower gasification rate than the other cases involving non-cooled WP, and it also has the lowest gasification rate among the cooled WP and the non-cooled WC. This can be explained by examining the char pore structure. The BS/IB chars were subjected to a relatively low heating rate during pyrolysis, as well as a low steam-char contact during char gasification, due to the blocking effect of the bed material. This ought to result in relatively compact, less reactive chars with a higher resistance to internal diffusion than for the other chars of the same fuel categories. This notion is supported by comparing the fractions of micropore area in Table 4.1, which are 1.3–2.0 times higher for the chars from Exps. 4, 8, and 12 than for the same types of char in the other experiments.

Table 4.1. Degree of char conversion, BET surface area, and the fraction of micropore area after 25 minutes of char gasification of wood pellets and wood chips that were subjected to different boundary conditions.

Exp.	Fuel	Boundary conditions	Degree of char conversion (%)	BET surface area (m ² /g)	Fraction of micropore area (-)
2	WP	IB/IB	87	1334	0.17
4	WP	BS/IB	63	1169	0.22
5	WP	BS/BS	87	1581	0.11
7	WP	IB/BS	88	1493	0.15
8	WP	BS/IB	62	1231	0.19
9	WP	BS/BS	81	1224	0.11
11	WC	IB/IB	82	469	0.14
12	WC	BS/IB	73	489	0.23

Figure 4.4 shows the gasification rate as a function of the degree of char conversion for four different cases, all of which were conducted using a bed temperature of 855°C and a steam concentration of 89%_{vol} during char gasification. The fuel in the “base case” underwent pyrolysis in an atmosphere of pure N₂, using ten whole pellets. In the remaining three cases, one of these parameters was varied: a mixture of steam (89%_{vol}) and N₂ (11%_{vol}) was used during pyrolysis; five pellets were used instead of ten; or the pellets were crushed prior to pyrolysis.

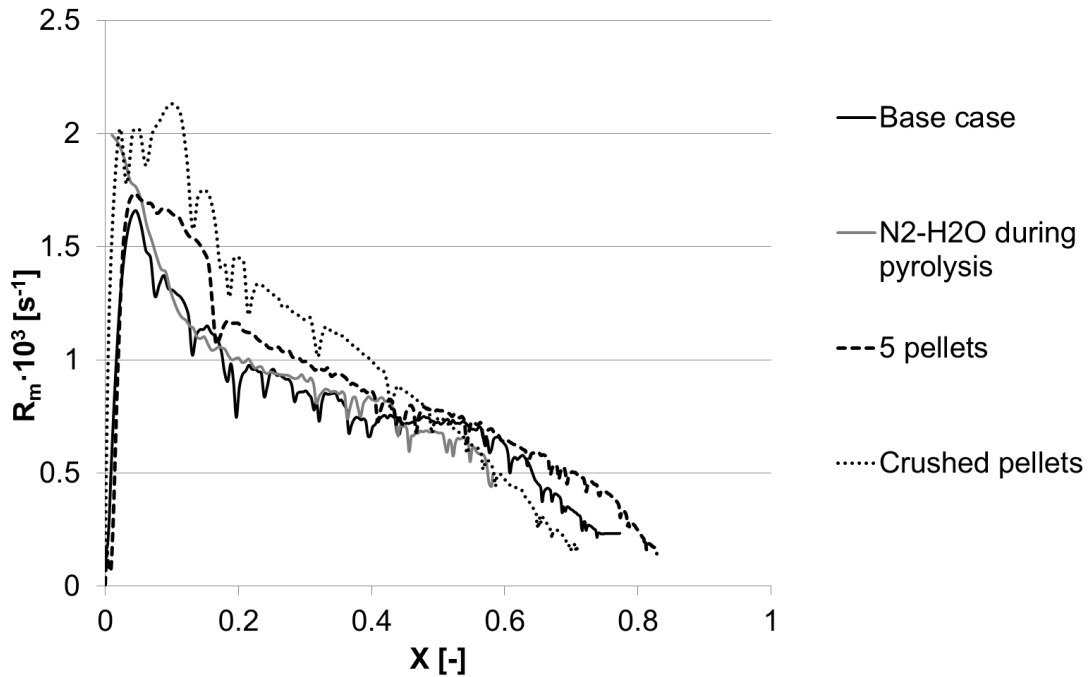


Figure 4.4. Gasification rate as a function of the degree of char conversion for different pyrolysis atmospheres, number of pellets, and fuel particle size.

As can be seen in Fig. 4.4, crushing the pellets had the greatest impact on the gasification rate, both quantitatively (the smaller the size, the higher the rate) and with respect to its dependence on the degree of conversion. The higher gasification rate of the crushed pellets can to some extent be attributed to the lower resistance to steam diffusion exhibited by smaller particles, as compared to larger particles. However, in the work conducted by Lundberg et al. [51], diffusion effects seemed to disappear at $X > 20\%$ for the conditions used in the experiments presented in Fig. 4.4. In addition to diffusional effects, the smaller particles were subjected to a higher heating rate during pyrolysis, which increases the char reactivity, as discussed in Section 1.2.2. The gasification rate was not affected by the pyrolysis atmosphere, whereas it increased somewhat when the number of pellets (i.e., the fuel concentration) was decreased. The influence of the number of pellets on the gasification rate may be explained by inherent variations in the fuel composition [52], which become more prominent when smaller batches of pellets are used. In parallel, a lower fuel concentration reduces the amount of H_2 in the surrounding gas, and thereby, decreases the level of H_2 inhibition, which results in a higher gasification rate [21].

As the operational conditions of a DFBG system can influence the fuel mixing, and thereby, the vertical distribution of fuel particles and the environment to which the particles are exposed, they can have an effect on the maximal char gasification rate (in the absence of volatile species). Consequently, in char reactivity tests, it is important to replicate the conditions under which the char is generated and gasified at the desired end-scale, using similar fuel sizes. Furthermore, in such tests, cooling the char prior to char gasification should be avoided, as this decreases the char reactivity.

In order to improve the modelling of the fuel conversion, a conversion class model was developed and evaluated in Paper 2. Figure 4.5 shows how the error, ε_k [defined in Eq. (16) in Paper 2], depends on the number of classes, N_k , using: a) the simple method of setting the value of $\Delta X_{j,k}$ equally high (Fig. 2.4a); and b) the proposed method based on setting all values of $A_{j,k}$ equally high (Fig. 2.4b). As seen in Fig. 4.5b, to achieve an error of less than 5%, three classes are sufficient to describe the drying and char gasification, whereas four classes are needed to describe the pyrolysis, using the proposed method. Comparing Figs. 4.5a and 4.5b, it is evident that the error is significantly (up to 10-fold) larger when equally large classes are used, especially for pyrolysis, for which as many as ten classes are required to achieve an error below 5%. It should also be noted that the use of only one class (equivalent to using constant rates), results in large errors (25%–37%), which can be reduced significantly by introducing a few extra conversion classes.

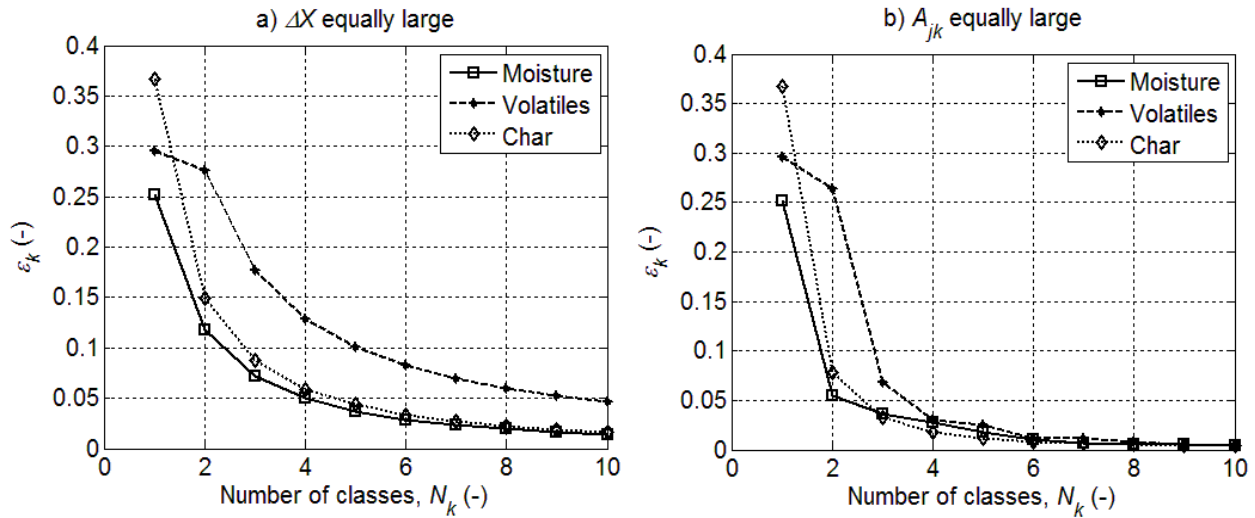


Figure 4.5. The error as a function of the number of classes used for the three stages of fuel conversion at 800°C for: a) when the $\Delta X_{j,k}$ values are equally high; and b) the proposed method with equally high values of $A_{j,k}$.

The conversion class model was combined with the determined kinetic and structural parameters and incorporated into the 1D model. Figure 4.6 shows how the degree of char conversion depends on the number of char conversion classes used for the two cases described in Section 2.1.2. As seen, when only one class is used, the degree of char conversion is strongly under-predicted for both cases. It then increases with the number of classes used, but after 4–6 classes, the change is less prominent, and the degree of char conversion stabilises at around 6% for the Chalmers gasifier and at around 71% for the larger gasifier.

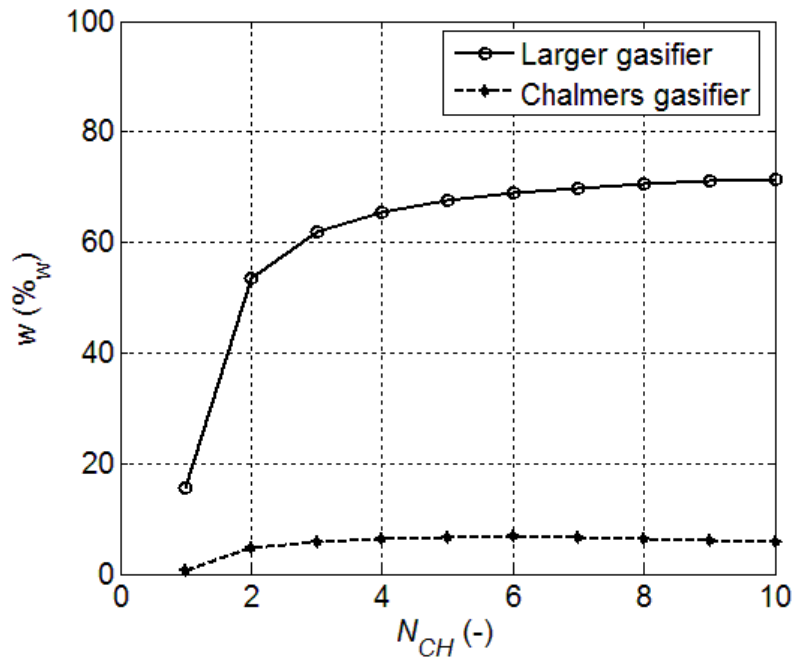


Figure 4.6. Dependency of the modelled degree of char conversion in the gasification chamber on the number of char classes used.

Figure 4.7 shows the dependence of the degree of char conversion on the recirculation of the bed material, as predicted by the 1D model, for $K_{be} = 10 \text{ s}^{-1}$.

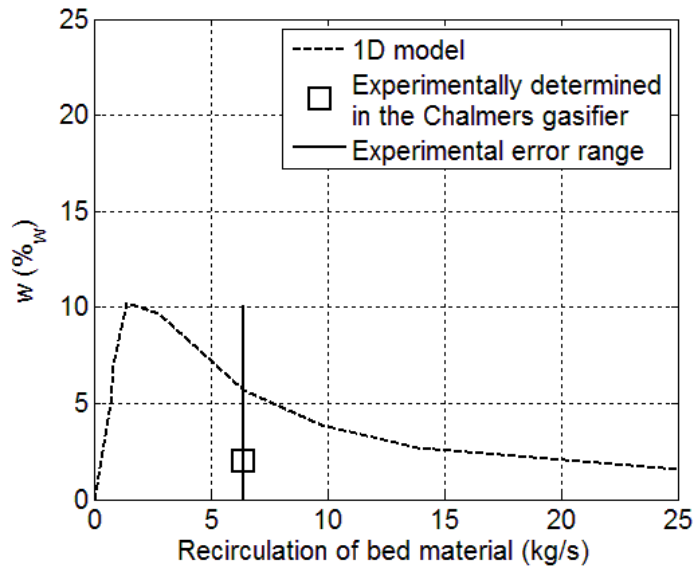


Figure 4.7. Degree of char conversion in the Chalmers gasifier as a function of the recirculation of the bed material. $K_{be} = 10 \text{ s}^{-1}$.

As seen, the degree of char conversion predicted by the 1D model is now within the margin of error of the experimental char conversion degree (0%–10%), thus giving a much better fit than when literature data were used in combination with the shrinking sphere model (Fig. 4.1).

5. Conclusions

The effects of different parameters on the degree of fuel conversion in the gasifier of a DFBG unit have been investigated through modelling and experiments. The developed 1D model was used to investigate how the degree of char conversion in the Chalmers gasifier is influenced by different factors, among which the char reactivity was identified as a critical parameter. The model was able to predict a peak in the degree of char conversion at a specific bed material recirculation rate. The effect of gas-solids mixing on the char reactivity was found to increase with the biomass reactivity.

A suitable discretisation method was identified for the conversion classes used in the population balances for modelling fuel conversion. The developed method was subsequently incorporated into the 1D model and used to model char conversion in large-scale units. Around 4–6 classes were needed to describe the char conversion in a satisfactory way, and the modelled char conversion degree was within the error margin of the experimentally determined value obtained using the Chalmers gasifier.

Furthermore, the influences of the fuel size and the surrounding conditions of a fuel particle on the char gasification rate were investigated experimentally. It was found that the fuel positions during pyrolysis and char gasification have a significant effect on the char gasification rate, for conditions relevant for DFBG; when pyrolysis on the bed surface was followed by char gasification inside the dense bed, the char gasification rate was up to 2-fold lower than it was for the other three studied combinations, all of which yielded similar char gasification rates. Cooling the char after pyrolysis decreased the char gasification rate for all the cases studied, whereas the pyrolysis atmosphere had no significant effect on the char gasification rate. Fuel particle size was found to affect both the gasification rate (the smaller the particle size, the higher the rate) and its dependence on the degree of char conversion, in a way that could not be entirely explained by diffusional effects. Thus, when carrying out laboratory-scale tests to determine fuel reactivity data to be used in the modelling of a large-scale unit, it is important to replicate the conditions experienced by the fuel particles in the large-scale unit, using similar fuel particle sizes.

6. Future Work

As seen in Table 1.2, the effects of additional parameters on the degree of fuel conversion need to be determined. H₂ inhibition, ash effects, CO₂ gasification, and the gasification atmosphere are mentioned in Table 1.2, but this list should not be considered exhaustive. Furthermore, the 1D model will be validated using new data from the Chalmers gasifier and the GoBiGas project. The 1D model will also be developed into a 3D model, which will include the freeboard in the gasification chamber.

Notation

Roman letters			
a	parameter used in the EM (-)	k'	dispersion heat transfer coefficient (W/m/K)
A_j	error of class j (s)	k_0	pre-exponential factor ($\text{bar}^{-0.4}\text{s}^{-1}$)
b	parameter used in the EM (-)	K_{be}	bubble-emulsion interchange coefficient (s^{-1})
c	parameter used in the EM (-)	k_{rc}	rate constant of CG (m/s)
C_p	heat capacity (J/mole/K)	$k_{rc,eff}$	effective rate constant of CG (m/s)
D	dispersion coefficient (m^2/s)	$L_{Chalmers}$	length of the Chalmers gasifier (-)
d	parameter used in the EM (-)	lf	loss factor ($\text{J}/\text{J}_{\text{fuel}}$)
D_{AB}	binary diffusion coefficient (m^2/s)	LHV	lower heating value (J/mole)
d_p	particle diameter (m)	m	mass (kg)
E_a	activation energy (J/mole)	M	molar mass (kg/mole)
$f(X)$	structural model (-)	\dot{m}_j	mass flow leaving class j (kg/s)
h	enthalpy (J/kg)	m_C	mass of carbon (kg)
ΔH	heat of reaction (J/mole)	$m_{C,0}$	initial mass of carbon (kg)
h_m	mass transfer coefficient (m/s)	n	exponent of gaseous reactant (steam) (-)
k	thermal conductivity (W/m/K)	$n_{CO,0}$	initial number of moles of CO ($\text{mole}_{\text{CO}}/\text{mole}_{\text{F}}$)

$n_{H_2,0}$	initial number of moles of H ₂ (mole _{H2} /mole _F)	R	reaction rate (s ⁻¹)
N_k	number of classes of fuel component k (-)	R	gas constant (J/mole/K)
n_{RG}	molar flow of dry raw gas (mole _{RG} /mole _F)	R_m	conversion rate (s ⁻¹)
n_{shift}	moles shifted in WGS (mole _{shifted} /mole _F)	S	source term (depends on equation)
P_{H_2O}	partial pressure of steam (bar)	SFR	steam-to-fuel ratio (kg _S /kg _F)
q_{comb}	heat of combustion (J/mole _F)	T	temperature (K)
$q_{CH_4,out}$	potential heat content in CH ₄ (J/mole _F)	t	time (s)
q_{demand}	internal heat demand (J/mole _F)	u	velocity (m/s)
q_{dev}	heat of devolatilisation (J/mole _F)	w	degree of char conversion in gasifier (-)
$q_{heat,A}$	demand for heating air (J/mole _{fuel})	X	degree of conversion (-)
$q_{heat,F}$	demand for heating fuel (J/mole _{fuel})	x	space coordinate (m)
$q_{heat,RG}$	demand for heating raw gas (J/mole _{fuel})	x	fraction reacting in R.A1 (-)
$q_{heat,S}$	demand for heating steam (J/mole _{fuel})	ΔX_j	size of class j (-)
q_{gasif}	heat of char gasification (J/mole _{fuel})	Y	gas mass fraction (kg/kg)
$q_{loss,W}$	heat loss through walls (J/mole _{fuel})	y	fraction of recirculated gas (-)
q_{shift}	heat of WGS reaction (J/mole)	z	part of remaining fuel reacting in R.A2 (-)

Greek letters		Dimensionless numbers	
γ	H ₂ /CO ratio (mole H ₂ /mole CO)	Re	Reynolds number (-)
ε_k	error of fuel component k	Sc	Schmidt number (-)
η_{SNG}	overall SNG efficiency (kJ/kJ _{fuel})	Sh	Sherwood number (-)
θ	cross-flow impact factor (-)		
ρ	mass concentration (kg/m ³)	Acronyms	
Φ	potential flow function (kg/m ³)	BET	Brunauer–Emmett–Teller
ψ	parameter used in the RPM (-)	BFB	bubbling fluidised bed
		BS	bed surface
Indices		CG	char gasification
20	20% char conversion	CFB	circulating fluidised bed
A	air	CFD	computational fluid dynamics
b	bubble phase	$DFBG$	dual fluidised bed gasification
BM	bed material	DME	dimethyl ether
c	combustor	EFG	entrained flow gasification
CH	char	EM	empirical model
$conv$	conversion	F	free
e	emulsion phase	FB	fluidised bed
E	energy	FBG	(single) fluidised bed gasification
F	fuel	GM	grain model
G	gas	IB	inside dense bed
g	gasifier	$IGCC$	integrated gasification combined cycle
i	gas species	LHS	left-hand side
in	inlet	LPT	Lagrangian particle tracking
j	conversion class	P	pyrolysis
k	fuel component	RHS	right-hand side
p	products	RPM	random pore model
RG	raw gas	SNG	substitute natural gas
r	reactants	WC	wood chips
S	steam	WGS	water gas shift
		WP	wood pellets

References

- [1] Trafikverket. Transportsektorns utsläpp. <http://www.trafikverket.se/Privat/Miljo-och-halsa/Klimat/Transportsektorns-utslapp/2014-04-02>.
- [2] Hofbauer H. Scale Up of Fluidized Bed Gasifiers from Laboratory Scale to Commercial Plants: Steam Gasification of Solid Biomass in a Dual Fluidized Bed System. FBC19. Vienna 2006.
- [3] Neubauer Y. 6 - Biomass gasification. In: Rosendahl L, editor. Biomass Combustion Science, Technology and Engineering: Woodhead Publishing; 2013. p. 106-29.
- [4] Larsson A. Fuel conversion in a dual fluidized bed gasifier -experimental quantification and impact on performance: Chalmers University of Technology; 2014.
- [5] Larsson A, Seemann M, Neves D, Thunman H. Evaluation of performance of industrial-scale dual fluidized bed gasifiers using the chalmers 2-4-MWth gasifier. Energy Fuels. 2013;27:6665-80.
- [6] Tengberg F, Gunnarsson, I. Progress Report 7 GoBiGas. Göteborg: Göteborg Energi; 2015.
- [7] Tchhoffor PA, Davidsson KO, Thunman H. Transformation and release of potassium, chlorine, and sulfur from wheat straw under conditions relevant to dual fluidized bed gasification. Energy Fuels. 2013;27:7510-20.
- [8] Gómez-Barea A, Leckner B. Modeling of biomass gasification in fluidized bed. Progress in Energy and Combustion Science. 2010;36:444-509.
- [9] Kunii D, Levenspiel, O. Fluidization Engineering. Newton: Butterworth-Heinemann; 1991.
- [10] Di Blasi C. Combustion and gasification rates of lignocellulosic chars. Progress in Energy and Combustion Science. 2009;35:121-40.
- [11] Cetin E, Moghtaderi B, Gupta R, Wall TF. Influence of pyrolysis conditions on the structure and gasification reactivity of biomass chars. Fuel. 2004;83:2139-50.
- [12] Chen G, Yu Q, Sjöström K. Reactivity of char from pyrolysis of birch wood. Journal of Analytical and Applied Pyrolysis. 1997;40-41:491-9.
- [13] Fushimi C, Araki K, Yamaguchi Y, Tsutsumi A. Effect of heating rate on steam gasification of biomass. 1. Reactivity of char. Ind Eng Chem Res. 2003;42:3922-8.
- [14] Kumar M, Gupta RC. Influence of carbonization conditions on the gasification of acacia and eucalyptus wood chars by carbon dioxide. Fuel. 1994;73:1922-5.
- [15] Mermoud F, Salvador S, Van de Steene L, Golfier F. Influence of the pyrolysis heating rate on the steam gasification rate of large wood char particles. Fuel. 2006;85:1473-82.

- [16] Tchoffor PA, Davidsson, K. Effects of Steam on the Release of Potassium, Chlorine, and Sulfur during Char Conversion, Investigated under Dual-Fluidized-Bed Gasification Conditions. *Energy Fuels*. 2014;Fuel 28 6953–65.
- [17] Nilsson S, Gómez-Barea A, Cano DF. Gasification reactivity of char from dried sewage sludge in a fluidized bed. *Fuel*. 2012;92:346-53.
- [18] Nilsson S, Gómez-Barea A, Fuentes-Cano D, Campoy M. Gasification kinetics of char from olive tree pruning in fluidized bed. *Fuel*. 2014;125:192-9.
- [19] Nilsson S, Gómez-Barea A, Ollero P. Gasification of char from dried sewage sludge in fluidized bed: Reaction rate in mixtures of CO₂ and H₂O. *Fuel*. 2013;105:764-8.
- [20] Moilanen A, Mühlen H-J. Characterization of gasification reactivity of peat char in pressurized conditions: Effect of product gas inhibition and inorganic material. *Fuel*. 1996;75:1279-85.
- [21] Barrio M, Gøbel, B., Risnes, H., Henriksen, U., Hustad, J.E., Sørensen, L.H. Steam gasification of wood char and the effect of hydrogen inhibition on the chemical kinetics. In: Bridgwater AV, editor. *Progress in Thermochemical Biomass Conversion*. U.K.: Blackwell Science; 2001.
- [22] Fushimi C, Wada T, Tsutsumi A. Inhibition of steam gasification of biomass char by hydrogen and tar. *Biomass and Bioenergy*. 2011;35:179-85.
- [23] Peng FF, Lee IC, Yang RYK. Reactivities of in situ and ex situ coal chars during gasification in steam at 1000–1400°C. *Fuel Processing Technology*. 1995;41:233-51.
- [24] Zhang R, Wang Q, Luo Z, Fang M. Effect of pyrolysis atmosphere and temperature on coal char gasification reactivity. 11th International Conference on Fluidized Bed Technology, CFB 2014. Beijing: Chemical Industry Press; 2014. p. 667-72.
- [25] Slaghuis JH, van der Walt TJ. Increased reactivity of char due to pyrolysis in a reactive atmosphere. *Fuel*. 1991;70:831-4.
- [26] Li F-h, Li Z-z, Huang J-j, Fang Y-t. Characteristics of fine chars from fluidized bed gasification of Shenmu coal. *Journal of Fuel Chemistry and Technology*. 2014;42:1153-9.
- [27] Berdugo Vilches T, Sette, E., Thunman, H. Behaviour of biomass particles in a large scale (2-4MWth) bubbling bed reactor. *Multiphase Flow 2015*. València, Spain 2015.
- [28] de Souza-Santos ML. Basic Remarks on Modeling and Simulation. *Solid Fuels Combustion and Gasification*: CRC Press; 2010. p. 1-17.
- [29] Pallarès D. Fluidized bed combustion -modelling and mixing. Göteborg: Chalmers University of Technology; 2008.

- [30] Myöhänen K. Modelling of combustion and sorbent reactions in three-dimensional flow environment of a circulating fluidized bed furnace: Lappeenranta University of Technology; 2011.
- [31] Ratschow L. Three-Dimensional Simulation of Temperature Distributions in Large-Scale Circulating Fluidized Bed Combustors: Technical University of Hamburg-Harburg; 2009.
- [32] Nikoo MB, Mahinpey N. Simulation of biomass gasification in fluidized bed reactor using ASPEN PLUS. *Biomass and Bioenergy*. 2008;32:1245-54.
- [33] Jiang H, Morey RV. A numerical model of a fluidized bed biomass gasifier. *Biomass and Bioenergy*. 1992;3:431-47.
- [34] Radmanesh R, Cnaouki J, Guy C. Biomass gasification in a bubbling fluidized bed reactor: Experiments and modeling. *AIChE J*. 2006;52:4258-72.
- [35] Petersen I, Werther J. Three-dimensional modeling of a circulating fluidized bed gasifier for sewage sludge. *Chemical Engineering Science*. 2005;60:4469-84.
- [36] Sofialidis D, Faltsi, O. Simulation of biomass gasification in fluidized beds using computational fluid dynamics approach. *Thermal Science* 2001;5:95-105.
- [37] Oevermann M, Gerber S, Behrendt F. Euler-euler and euler-lagrange modeling of wood gasification in fluidized beds. 9th International Conference on Circulating Fluidized Beds, CFB 2008, in Conjunction with the 4th International VGB Workshop on Operating Experience with Fluidized Bed Firing Systems. Hamburg: TuTech Innovation GmbH; 2008.
- [38] Wang Y, Yan L. CFD modeling of a fluidized bed sewage sludge gasifier for syngas. *Asia-Pac J Chem Eng*. 2008;3:161-70.
- [39] Ravelli S, Perdichizzi A, Barigozzi G. Description, applications and numerical modelling of bubbling fluidized bed combustion in waste-to-energy plants. *Progress in Energy and Combustion Science*. 2008;34:224-53.
- [40] Hannes JP. Mathematical Modelling of Circulating Fluidized Bed Combustion: Technical University of Delft; 1996.
- [41] Jennen T, Hiller R, Köneke D, Weinspach PM. Modeling of gasification of wood in a circulating fluidized bed. *Chem Eng Technol*. 1999;22:822-6.
- [42] Toomey RD, Johnstone, H.F. Gaseous fluidization of solid particles. *Chemical Engineering Progress*. 1952;48:220-5.
- [43] Sette E, Pallarès D, Johnsson F. Influence of bulk solids cross-flow on lateral mixing of fuel in dual fluidized beds. *Fuel Processing Technology*. 2015;140:245-51.
- [44] Johansson R, Thunman H, Leckner B. Influence of intraparticle gradients in modeling of fixed bed combustion. *Combustion and Flame*. 2007;149:49-62.

- [45] Palchonok G. Heat and Mass Transfer to a Single Particle in Fluidized Bed. Göteborg, Sweden: Chalmers University of Technology; 1998.
- [46] Tamarin AI. Model of Coal Combustion in a Fluidized Bed and its Experimental Identification. Journal of Engineering Physics and Thermodynamics. 1991;60:693-7.
- [47] Ranz WE. Friction and Heat Transfer Coefficient for Single Particles and Packed Beds. Chemical Engineering Progress. 1952;27:247-53.
- [48] Lu GQ, . Do, D.D. Comparison of structural models for high-ash char gasification. Carbon 1994;32:247-63.
- [49] Ishida M, Wen, C.Y. Comparison of zone-reaction model and unreacted-core shrinking model in solid-gas reactions - I Isothermal analysis. Chemical Engineering Science. 1971;26: 1031-41.
- [50] Bhatia SK, Perlmutter, D.D. A random pore model for fluid-solid reactions: I. Isothermal, kinetic control. AIChE Journal. 1980;26:379–86.
- [51] Lundberg L, Tchoffor, P.A., Johansson, R., Pallarès, D. Determination of Kinetic Parameters for the Gasification of Biomass Char Using a Bubbling Fluidised Bed Reactor. 22nd International Conference on Fluidized Bed Conversion. Turku, Finland 2015.
- [52] Qin K, Thunman H. Diversity of chemical composition and combustion reactivity of various biomass fuels. Fuel. 2015;147:161-9.
- [53] Thunman H, Niklasson F, Johnsson F, Leckner B. Composition of volatile gases and thermochemical properties of wood for modeling of fixed or fluidized beds. Energy Fuels. 2001;15:1488-97.

Appendix A: Calculation of the Overall Efficiency of the DFBG Process for SNG Production

The equations and data used in the example calculation of the overall efficiency of the DFBG process for SNG production (Fig. 1.2) are presented in this section. The overall efficiency of SNG production, η_{SNG} , is given by the energy content of the methane leaving the system boundaries in Fig. 1.1 [$q_{CH_4,out}$, Eq. (A2)], divided by the energy content of the biomass:

$$\eta_{SNG} = \frac{q_{CH_4,out}}{LHV_F} \quad (A1)$$

The biomass is here represented by $C_{1.5}H_2O$ (approximately corresponding to the compositions of the WP and WC given in Paper 2) and the decomposition of the fuel is assumed to take place according to R.A1–R.A3 (Table A1), as schematised in Fig. A1. The specific conversion steps illustrated in Fig. A1 are chosen to simplify the calculations and consist of the following: in R.A1, a fraction x of the biomass decomposes into char ($C_{1.5}$) and steam; the remaining biomass, $(1-x)$, forms CH_4 and CO_2 through R.A2, or CO and H_2 through R.A3. While z is the fraction of the biomass remaining after R.A1 that reacts through R.A2, $(1-z)$ is the fraction that undergoes R.A3. The values for x and z were chosen to give a reasonable char yield (15%_{dar}) and a realistic composition of the volatile gases (see Fig. 1.3 at $w = 0$).

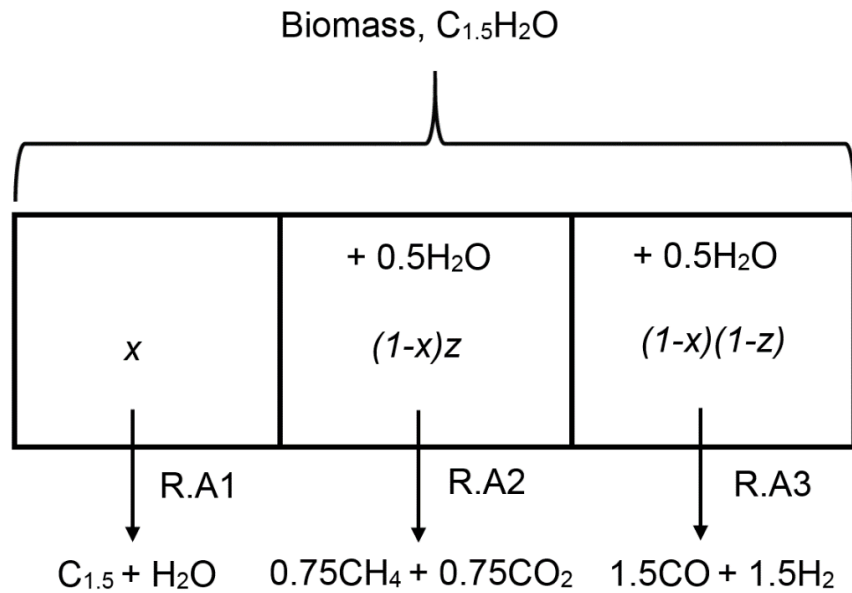


Figure A1. Schematic of the decomposition process for biomass.

A fraction w of the char formed in R.A1 can subsequently undergo char gasification (R.A4). Furthermore, the gas species can undergo the WGS reaction (R.A5) and the methanation reaction (R.A6). Adding R.A5 to R.A6 and multiplying by 0.75 yields the overall reaction given by R.A7. This reaction expresses how the products from R.A3 and R.A4 can be converted into CO_2 and CH_4 , which will maximise the methane production.

Table A1. Reactions used in the example.

Reaction	Heat of reaction (kJ/mole)	Reaction no.
$C_{1.5}H_2O \rightarrow C_{1.5} + H_2O$	$\{\Delta H_1 = LHV_{p,1} - LHV_F\}$	(R.A1)
$C_{1.5}H_2O + 0.5H_2O \rightarrow 0.75CH_4 + 0.75CO_2$	$\{\Delta H_2 = LHV_{p,2} - LHV_F\}$	(R.A2)
$C_{1.5}H_2O + 0.5H_2O \rightarrow 1.5CO + 1.5H_2$	$\{\Delta H_3 = LHV_{p,3} - LHV_F\}$	(R.A3)
$C_{1.5} + 1.5H_2O \rightarrow 1.5CO + 1.5H_2$	$\{\Delta H_4 = LHV_{p,4} - LHV_{r,4}\}$	(R.A4)
$CO + H_2O \leftrightarrow CO_2 + H_2$	$\{\Delta H_5\}$	(R.A5)
$3H_2 + CO \leftrightarrow CH_4 + H_2O$	$\{\Delta H_6\}$	(R.A6)
$1.5CO + 1.5H_2 \leftrightarrow 0.75CO_2 + 0.75CH_4$	$\{0.75 \cdot (\Delta H_5 + \Delta H_6) = LHV_{p,2} - LHV_{p,3}\}$	(R.A7)

The maximal energy content of methane leaving the system is thus given by:

$$q_{CH_4,out} = \left((1-x) \cdot LHV_{p,2} + x \cdot w \cdot LHV_{p,2} \right) \cdot (1-y) \quad (\text{A2})$$

In Eq. (A2), y is the fraction of gas that is recirculated to the combustion chamber. As seen, $q_{CH_4,out}$ contains both the heat content of the CH_4 formed in R.A2 and the heat content of the CH_4 that potentially can be formed by CO and H_2 (R.A3 and R.A4, through R.A7) in the shifting and methanation steps outside the system boundaries, and therefore gives the maximum efficiency when inserted into Eq. (A1). As seen in Eqs. (A1) and (A2), the overall efficiency depends on the fraction of recirculated raw gas, y . To calculate y , a heat balance can be set up, in which the internal heat demand of the processes within the system boundaries shown in Fig. 1.1., q_{demand} , has to be covered by combustion of the char remaining after gasification and combustion of the raw gas, q_{comb} :

$$q_{demand} = q_{comb} \quad (\text{A3})$$

The internal heat demand is divided into one loss term, four terms related to the heating of steam, fuel, air, and recirculated raw gas, respectively, and three reaction terms:

$$q_{demand} = q_{loss,W} + q_{heat,S} + q_{heat,F} + q_{heat,A} + q_{heat,RG} + q_{dev} + q_{gasif} + q_{shift} \quad (\text{A4})$$

Here, q_{shift} is the heat required by the WGS reaction that occurs within the gasification chamber. As methanation (and if necessary, additional shifting) takes place outside the system boundaries, these processes are not included in the internal heat balance [Eq. (A3)]. Table A2 summarises the loss terms and reaction terms in Eq. (A4).

Table A2. Definitions of the loss, heat demands, and reaction terms in Eq. (A4) (kJ/mole_{fuel}).

	Description	Equation	Name
$q_{loss,W}$	Heat loss through walls of system	$lf \cdot LHV_F$	(A5)
$q_{heat,S}$	Demand for heating steam to T_g	$SFR \cdot M_S \cdot C_{P,S} \cdot (T_g - T_{S,in})$	(A6)
$q_{heat,F}$	Demand for heating fuel to T_g	$M_F \cdot C_{P,F} \cdot (T_g - T_{F,in})$	(A7)
$q_{heat,A}$	Demand for heating air to T_c	$[y \cdot (1 - x + x \cdot w) + x \cdot (1 - w)] \cdot 1.5 \cdot 4.77 \cdot C_{p,A} \cdot (T_c - T_{A,in})$	(A8)
$q_{heat,RG}$	Demand for heating recirculated gas to T_c	$n_{RG} \cdot y \cdot C_{p,RG} \cdot (T_c - T_{RG,in})$	(A9)
q_{dev}	Heat of devolatilisation	$x \cdot \Delta H_1 + (1 - x) \cdot (z \cdot \Delta H_2 + (1 - z) \cdot \Delta H_3)$	(A10)
q_{gasif}	Heat of char gasification	$x \cdot w \cdot \Delta H_4$	(A11)
q_{shift}	Heat of the WGS reaction	$n_{shift} \cdot \Delta H_5$	(A12)

The loss term, $q_{loss,W}$, corresponds to the heat lost through the walls of the system; it is assumed that 5% (= lf) of the heat content of the fuel is lost in this way. The second and third terms in Eq. (A4) are related to heating the steam and fuel to the temperature of the gasifier, whereas the fourth and fifth terms describe heating of the air and recirculated raw gas to the temperature of the combustor (the recirculated raw gas is cooled prior to entering the combustion chamber for practical reasons, e.g., pressurisation). In Eq. (A9), n_{RG} (mole_{RG}/mole_F) is the relative molar flow of dry raw gas exiting the gasifier:

$$n_{RG} = 3 \cdot ((1 - x) \cdot (1 - z) + w \cdot x) + 1.5 \cdot (1 - x) \cdot z + \frac{q_{shift}}{\Delta H_5} \quad (A13)$$

The number 3 in Eq. (A13) comes from the number of moles of products in R.A3 and R.A4: $1.5 + 1.5 = 3$. Likewise, 1.5 is the total number of moles formed in R.A2 ($0.75 + 0.75 = 1.5$). The last term describes the number of moles of H₂O being converted to H₂ in the WGS reaction.

Equations (A10)–(A12) describe the heat produced or consumed during devolatilisation, char gasification, and in the WGS reaction. In Eq. (A12), n_{shift} is the number of moles shifted in the WGS reaction per mole of biomass. For a certain H_2/CO ratio, γ , n_{shift} is given by:

$$\frac{n_{H_2,0} + n_{shift}}{n_{CO,0} - n_{shift}} = \frac{1.5 \cdot ((1-x) \cdot (1-z) + w \cdot x) + n_{shift}}{1.5 \cdot ((1-x) \cdot (1-z) + w \cdot x) - n_{shift}} = \gamma \quad (A14a)$$

$$\rightarrow n_{shift} = 1.5 \cdot ((1-x) \cdot (1-z) + w \cdot x) \cdot \frac{\gamma - 1}{\gamma + 1} \quad (A14b)$$

As described above, the heat demand is met by the combustion of char and a part of the raw gas:

$$q_{comb} = x \cdot (1-w) \cdot LHV_{p,1} + y \cdot ((1-x) \cdot (z \cdot LHV_{p,2} + (1-z) \cdot LHV_{p,3}) + x \cdot w \cdot LHV_{p,4} - q_{shift}) \quad (A15)$$

Inserting Eqs. (A5)–(A14) into Eq. (A4), and setting Eq. (A4) equal to Eq. (A15), the necessary fraction of recirculated raw gas, y , can be calculated, making it possible to calculate the overall efficiency using Eq. (A1). The data used to calculate η_{SNG} in Fig. 1.2 are given in Table A3.

Table A3. Parameters used in the given example.

	Description	Value/equation	Unit
$C_{P,A}$	Heat capacity of air	0.034	$\text{kJ}_A/(\text{mole}_A \cdot \text{K})$
$C_{P,F}$	Heat capacity of fuel [53]	$(4.206 \cdot \overline{T}_F - 37.7) \frac{M_F}{1000}$	$\text{kJ}_F/(\text{mole}_F \cdot \text{K})$
$C_{P,RG}$	Heat capacity of recirculated gas	0.035	$\text{kJ}_{RG}/(\text{mole}_{RG} \cdot \text{K})$
$C_{P,S}$	Heat capacity of steam	0.038	$\text{kJ}_S/(\text{mole}_S \cdot \text{K})$
lf	Loss factor through walls	0.05	$\text{kJ}_{\text{loss}}/\text{kJ}_F$
ΔH_5	Heat of WGS reaction	-41	$\text{kJ}/\text{mole}_{\text{shift}}$
LHV_F	LHV of fuel	675	$\text{kJ}_F/\text{mole}_F$
$LHV_{p,1}$	LHV of products in R.A1	590	$\text{kJ}_{p,1}/\text{mole}_F$
$LHV_{p,2}$	LHV of products in R.A2	602	$\text{kJ}_{p,2}/\text{mole}_F$
$LHV_{p,3,4}$	LHV of products in R.A3 and R.A4	787	$\text{kJ}_{p,3,4}/\text{mole}_F$
$LHV_{r,4}$	LHV of reactants in R.A4	590	$\text{kJ}_{r,4}/\text{mole}_F$
M_F	Molar mass of fuel	0.036	$\text{kg}_F/\text{mole}_F$
M_S	Molar mass of steam	0.018	$\text{kg}_S/\text{mole}_S$
SFR	Steam-to-fuel ratio	0.8	kg_S/kg_F
$T_{A,in}$	Air inlet temperature	773	K
T_c	Combustor temperature	1173	K
$T_{F,in}$	Fuel inlet temperature	298	K
T_g	Gasifier temperature	1103	K
$T_{RG,in}$	Inlet temperature of recirculated gas	323	K
$T_{S,in}$	Steam inlet temperature	140	K
x	See Fig. A1	0.3	-
z	See Fig. A1	0.5	-
γ	H_2/CO ratio	0.7, 1.0 and 3.0	$\text{mole}_{\text{H}_2}/\text{mole}_{\text{CO}}$